How to cite: *Angew. Chem. Int. Ed.* **2023**, *62*, e202308241
doi.org/10.1002/anie.202308241

Photochemistry

Catalytic Photochemical Deracemization via Short-Lived Intermediates

*Johannes Großkopf and Thorsten Bach**

Dedicated to Professor Manfred T. Reetz on the occasion of his 80th birthday

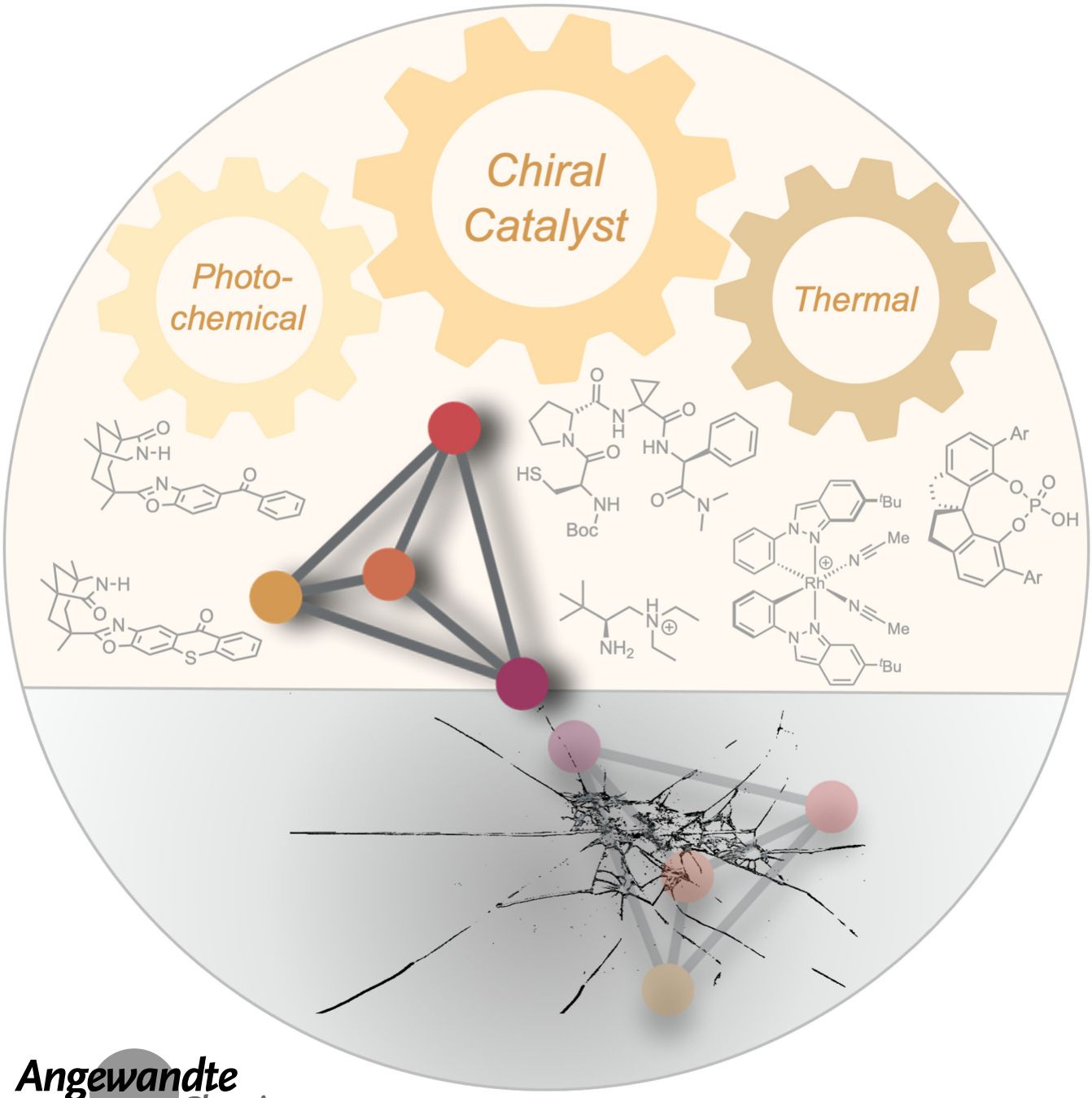

Abstract: Upon irradiation in the presence of a suitable chiral catalyst, racemic compound mixtures can be converted into enantiomerically pure compounds with the same constitution. The process is called photochemical deracemization and involves the formation of short-lived intermediates. By opening different reaction channels for the forward reaction to the intermediate and for the re-constitution of the chiral molecule, the entropically disfavored process becomes feasible. Since the discovery of the first photochemical deracemization in 2018, the field has been growing rapidly. This review comprehensively covers the research performed in the area and discusses current developments. It is subdivided according to the mode of action and the respective substrate classes. The focus of this review is on the scope of the individual reactions and on a discussion of the mechanistic details underlying the presented reaction.

1. Introduction

Photochemistry can change our perception of reactivity beyond the boundaries of conventional knowledge, because "the excited state opens reaction pathways that are not (or barely) accessible from the ground state".[1] In fact, the photon alters the energy profile of a reaction to the extent that fundamental considerations applicable to ground state reactions are challenged. It has become increasingly evident in recent years that contra-thermodynamic pathways can be photochemically unlocked[2] and the underlying reactions can be extremely useful tools in organic synthesis. Catalytic photochemical deracemization reactions represent one of the most, if not the most remarkable transformation of this type.[3] They revert a process which we intuitively consider as irreversible. Synthetic organic chemists are trained to be aware of conditions, which would potentially racemize a stereogenic center in a chiral compound. Thermodynamics would immediately punish the experimentalist who did not treat an enantiopure compound, e.g. an α-chiral amino acid derivative or an α-chiral aldehyde, with the required care. Attempts to recover a compound that had racemized were meant to fail in the same way as a gas would not spontaneously return once it had left a flask. Entropy favors statistically a racemic mixture over an enantiopure compound and racemization is inevitable in a thermal equilibrium. Photochemistry offers a straightforward way to compensate for the loss of entropy associated with a deracemization reaction and drives the equilibrium toward an enantiopure product.

Deracemization has been distinguished from kinetic resolution processes, which convert racemic substrates *rac*-**A** to structurally different products **B** (Scheme 1), and was defined as a reaction "in which a racemate is made nonracemic by increasing the quantity of one enantiomer at the expense of the other."[4] Although not included in this review, it is well established that the restrictions of thermodynamics can be thermally overcome by converting a chiral compound into an achiral intermediate which is subsequently re-converted by an enantioselective transformation.[5] Over the years, several thermal deracemization reactions were designed and successfully conducted which involve stable achiral intermediates, such as ketones and imines.[6]

Of course, photochemistry also needs to obey the fundamental rules of microscopic reversibility, i.e. that the initial half reaction (forward reaction) in a deracemization needs to be different from the second half reaction recovering the same compound.[7] The fascination of photochemical deracemization, as we know it today, relies on the creation of achiral intermediates which are short-lived and which cannot be exploited stoichiometrically in a thermal reaction. As such, it opens enantioselective access to unexplored product classes and can be extremely efficient due to

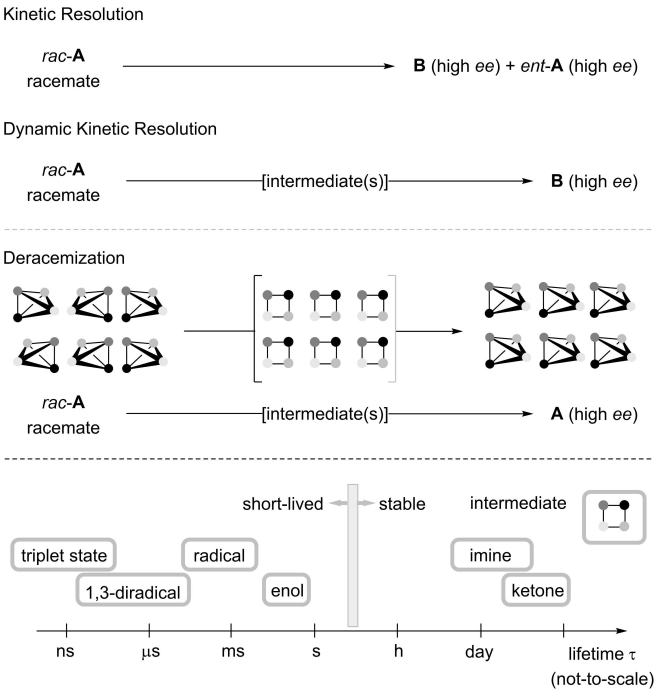

Scheme 1. Distinction between kinetic resolution, dynamic kinetic resolution, and deracemization (top); selection of representative intermediates in a deracemization and their rough order according to lifetime (bottom). Photochemical deracemization reactions typically involve short-lived achiral intermediates.

[*] Dr. J. Großkopf, Prof. Dr. T. Bach
School of Natural Sciences, Technische Universität München,
Department Chemie and Catalysis Research Center (CRC)
Lichtenbergstr. 4, 85747 Garching (Germany)
E-mail: thorsten.bach@ch.tum.de
Homepage: https://www.ch.nat.tum.de/oc1/startseite/

the rapid formation and decay of transient intermediates. In addition, photochemical deracemization allows for the use of a single catalyst under continuous reaction conditions since the individual steps occur on different hypersurfaces and the process does not violate the principle of microscopic reversibility.

In this review, the discussion focuses on photochemical deracemization reactions of organic compounds[8] which involve short-lived intermediates. Reactions, in which a stable intermediate was formed by a photochemical method or in which a stable intermediate was transformed photochemically,[9] are not included although they formally fulfill the criterion of a deracemization reaction. There is also not sufficient space to cover other methods which allow for the generation or isolation of enantiopure compounds from racemic mixtures.[10]

Although the distinction is fluid, we believe it useful to divide photochemical deracemization into two fundamentally different approaches (Scheme 2). In the first approach, a racemic mixture (represented by tetrahedrons with different chirality) is processed photochemically in the presence of a chiral photocatalyst. The photocatalyst enables a distinction between the two enantiomers, in a way that ideally one enantiomer is converted into an achiral short-lived intermediate (represented by a square). The intermediate decays thermally to the starting material, thus, avoiding microscopic reversibility. It is desirable that the achiral intermediate is detached from the photocatalyst before returning to the ground state. If so, it will statistically form the two enantiomers of the substrate while it would encounter an undesired bias if it remained bound. In the next catalytic cycle, the equilibrium is further shifted towards one of the two enantiomers until the mixture is eventually deracemized, i.e. enantiomer **A** prevails.

In an alternative approach, the photochemical step serves to form an achiral intermediate irrespective of the chirality of the starting material. The enantioselectivity stems from the subsequent thermal transformation of the intermediate which is promoted by a chiral catalyst. In cases in which the substrate is already bound to a chiral catalyst in the excitation process, the intermediate has lost its original

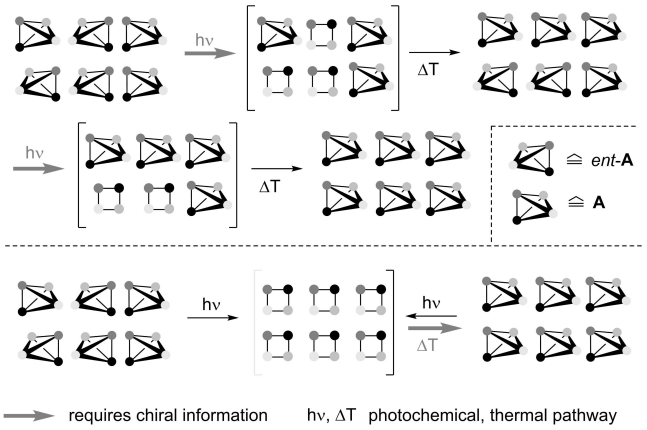

Scheme 2. Conceptually different approaches towards a catalytic photochemical deracemization: Selective processing of a single enantiomer (*ent*-**A**) by a chiral photocatalyst (top); selective processing of a photochemically generated, short-lived intermediate by a chiral catalyst (bottom). The tetrahedrons represent chiral molecules in both enantiomeric forms **A** and *ent*-**A**, the squares intermediates (see the text for details).

stereogenic element, but the complex with the catalyst is of course chiral. The thermal reaction must be compatible with the irradiation reaction, and it must be highly enantioselective to shift the equilibrium towards an enantiopure compound, i.e. to product enantiomer **A**. Consequently, the key interaction of the catalyst occurs with the intermediate, while in the first approach the catalyst interacts with the substrate but not necessarily with the intermediate.

Given that photochemical deracemization is a very recent development, several transient intermediates involved in the process have not been characterized by appropriate techniques. Still, we have provided the putative intermediate(s) in a separate drawing. The symbol for the intermediate (the square) is surrounded by dotted lines if it has not yet been detected and in bold lines if it has been spectroscopically identified.

Johannes Großkopf studied chemistry at the Technical University of Munich and the University of California, San Diego. During his Master's studies he spent three months in the group of Prof. R. Martín for a research internship at the ICIQ in Tarragona (Spain). In 2019 he received his M.Sc. degree, for which he was awarded the Manchot faculty prize. He performed his Ph.D. work as a fellow of the Fonds der Chemischen Industrie (Kekulé fellowship) in the group of Prof. T. Bach with a focus on the development of novel deracemization reactions. Recently, he joined the group of Prof. D. W. C. MacMillan (Princeton University) as a post-doctoral fellow funded by the German Academy of Sciences Leopoldina.

Thorsten Bach obtained his education at the University of Heidelberg and the University of Southern California, where he conducted his Diplom thesis with G. A. Olah. He received his Ph.D. in 1991 from the University of Marburg with M. T. Reetz and did postdoctoral work as a NATO fellow with D. A. Evans at Harvard University. He completed his Habilitation at the University of Münster in 1996, moved to the University of Marburg as an associate professor in 1997, and was appointed to the Chair of Organic Chemistry I at Technische Universität München in 2000. He is an elected member of the German Academy of Sciences Leopoldina since 2006 and the Bavarian Academy of Sciences since 2009. His research interests revolve around organic photochemistry, enantioselective catalysis, and natural product synthesis.

2. Rotation around Double Bonds

Olefins in an excited state of ππ* character, be it singlet or triplet, are configurationally unstable because rotation around the former double bond becomes feasible. The process has been extensively used for the contra-thermodynamic $E \rightarrow Z$ isomerization of alkenes[11] but it is also a suitable tool to promote deracemization reactions. Three major classes of olefins are covered in this section: allenes, axially chiral alkenes and enamines as intermediates in the deracemization of aldehydes.

2.1. Allenes

Multiply substituted allenes display an axis of chirality and are known to undergo racemization in their triplet state.[12] The first successful photochemical deracemization reaction, affording synthetically useful enantiomeric excesses, was reported in 2018 and employed thioxanthone **1**[13] as a single catalyst (Scheme 3).[14]

It was found that a broad variety of 3-(1′-alkenylidene)-piperidin-2-ones *rac*-**2** could be converted into enantioenriched products by simple visible light irradiation ($\lambda =$ 420 nm) in acetonitrile (Scheme 3). The functional group tolerance was high and allenes with a wide variety of substituents at the terminal position gave excellent results, typically with yields above 70 % and an enantiomeric excess (*ee*) exceeding 90 %. For allenes bearing only an aliphatic substituent (**2a**–**2d**) the reaction could be performed at room temperature, while additional functional groups (**2e**–**2h**) required irradiation at −40 °C to avoid side reactions.

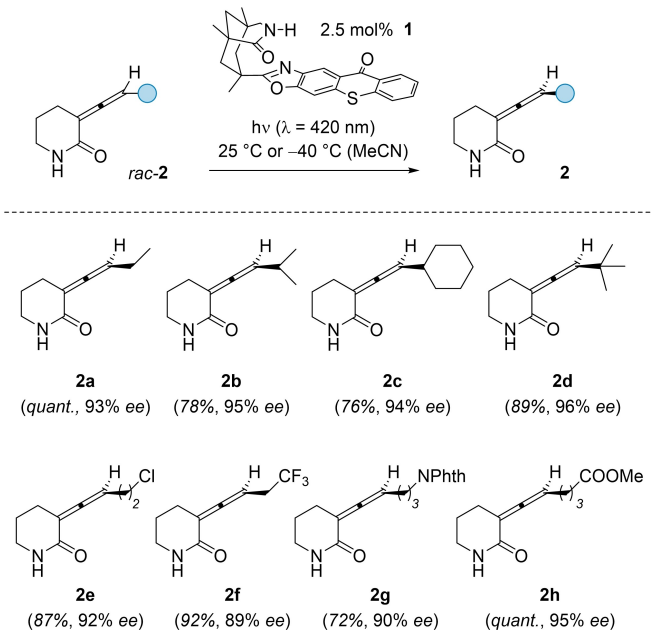

Scheme 3. Catalytic photochemical deracemization of 3-(1′-alkenylidene)piperidin-2-ones (*rac*-**2**) mediated by chiral thioxanthone **1**: Reaction conditions and a selection of products [Phth = phthaloyl].

Mechanistically, the deracemization of allenes follows the first approach described in Scheme 2. The absorption of the thioxanthone chromophore stretches into the visible region and it can transfer its triplet energy of $E_T =$ 263 kJ mol^{-1} (77 K, $PhCF_3$) to compound **2**. As for most aromatic carbonyl compounds, intersystem crossing (ISC) is rapid[15] and, thus, the photochemically relevant, excited thioxanthone **1*** is a triplet species. Triplet energy transfer is a viable pathway to promote an allene from the ground state to its triplet state.[14,16] The triplet energy of compound *rac*-**2d** was estimated by sensitization experiments to be in the order of $E_T \cong 250$ kJ mol^{-1}. Since we have recently elaborated on the mode of action of triplet energy transfer in more detail,[17] we keep the discussion on the topic short. Upon a spatially close encounter, thioxanthone **1*** can transfer its energy in an exothermic or even a slightly endothermic process to the allene (Scheme 4). The process is favored within substrate–catalyst complex **1**·*ent*-**2** for two reasons: Firstly, the complex forms with a higher association constant than **1**·**2**. Secondly, and more importantly, the chromophores are in much shorter distance (d) as calculated for the two enantiomers of compound *rac*-**2d**. The rate of energy transfer is proportional to e^{-d} (see below)[18] which in turn renders the formation of triplet intermediate **3** more rapid in the preferred cycle that involves *ent*-**2**.

Achiral intermediate **3** is best described as a diradical in which one unpaired electron resides in the sp^2-hydridized orbital of the central allene carbon atom and the other unpaired electron in the allylic π-orbital (one mesomeric form shown).[19] Decay of diradical **3** leads statistically to **2**

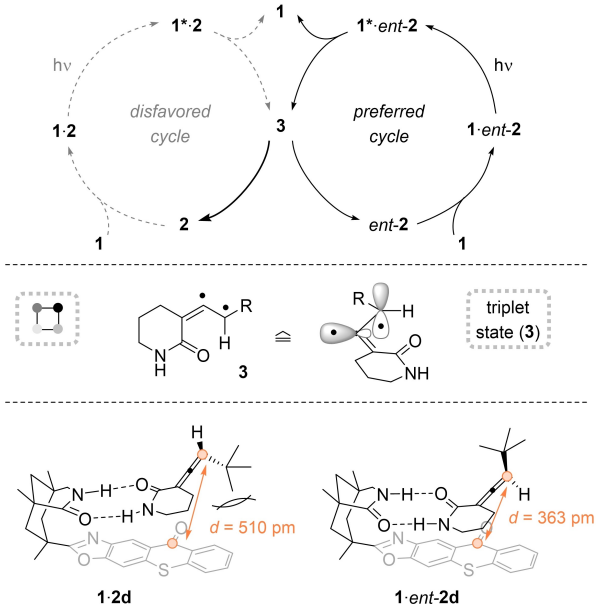

Scheme 4. Key features of the photochemical allene deracemization by triplet energy transfer: The chiral allene undergoes rotation upon energy transfer and forms the short-lived achiral triplet state (**3**). Upon decay to the ground state, allene enantiomers **2** and *ent*-**2** are generated from **3**. Enantiomer *ent*-**2** is preferentially processed which is due to preferred binding and due to the shorter distance of the chromophores (see text for details).

and *ent*-**2** provided that the diradical dissociates from the catalyst. In line with this, it was shown that the conversion of *ent*-**2** to preferred enantiomer **2** occurs with a quantum yield of 0.52, manifesting the high quantum efficiency of the deracemization reaction. A highly remarkable feature of this process is the fact that a single catalyst is responsible for the deracemization. The principle of microscopic reversibility is not violated because the forward reaction occurs photochemically while the re-formation of the allene from intermediate **3** takes place in the ground state. For cases where the enantioselectivity is less pronounced, it is likely a deviation from the idealistic scheme causing a lower enantiomeric excess. In addition, the allene might be prone to side reactions from its triplet state. Thioxanthone decomposition appears to be less significant, and the catalyst is still detectable at the end of the reaction.

In a second series of experiments, it was probed whether the five-membered pyrrolidinones *rac*-**4** would also be amenable to a similar differentiation by the chiral thioxanthone catalyst **1** (Scheme 5).[20] The compounds were found to be equally suited for a photochemical deracemization and delivered the desired products **4** with high enantioselectivity. It was established that the internal allene double bond underwent a Diels–Alder reaction which occurred *exo*-selectively with a high degree of chirality transfer (94–97 % *ee*). Bromine addition to the internal double bond was discovered to be another way to translate the axial chirality of the allenes into point chirality (91 % *ee*). Since binding of the five-membered pyrrolidinones to thioxanthone **1** follows the same pattern as for the piperidinones, it is assumed that the same mode of action applies (cf. Scheme 4).

When attempting the deracemization with a seven-membered 3-(3′,3′-dimethyl-1′-butenylidene)-azepan-2-one, a preference for one enantiomer was observed but the enantioselectivity dropped to 62 % *ee* compared to 98 % *ee* for **4a** and 96 % *ee* for **2d**. If the terminal position of the allene was not monosubstituted but substituted by a methyl and an ethyl group, a moderate enantioselectivity was observed in the deracemization reaction (45 % *ee*). Ring opening of the five-membered lactam ring in **4** to an acylic allene ketone was possible but turned out to be tedious. Against this background, an effort was made to utilize 2,4-disubstituted 2,3-butadienamides (allene amides) *rac*-**5** in a photochemical deracemization reaction, even though primary amides had shown inferior results in previous reactions[21] with chiral hydrogen-bonding catalysts or templates in comparison to their cyclic counterparts. Remarkably, the lactam-based thioxanthone **1** also allowed for a high enantioselectivity in this instance, with trifluorotoluene being the preferred solvent for the reaction (Scheme 6).[19b] The deracemization worked particularly well for substrates which displayed an arylmethyl group in 2-position and a bulky substituent at the terminal carbon atom C4 of the allene (products **5a**–**5f**). If the substituent at carbon atom C2 was an allyl (**5g**) or alkyl group (**5h**) the selectivity decreased.

Computational studies revealed that the triplet intermediate **6** involved in the reaction was structurally similar to the previously postulated intermediate **3** (Scheme 7). Its conformation was optimized for intermediate **6a** derived from allene *rac*-**5a**. Like for compounds *rac*-**2**, it is assumed that one enantiomer *ent*-**5** is processed much more efficiently by the catalyst than the major enantiomer **5** of the reaction. Triplet energy transfer is operative, and it was

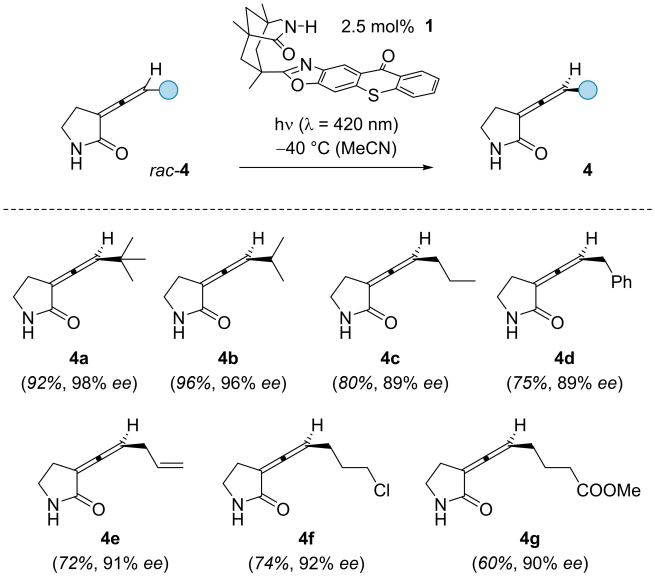

Scheme 5. Catalytic photochemical deracemization of 3-(1′-alkenylidene)-pyrrolidin-2-ones (*rac*-**4**) mediated by chiral thioxanthone **1**: Reaction conditions and a selection of products.

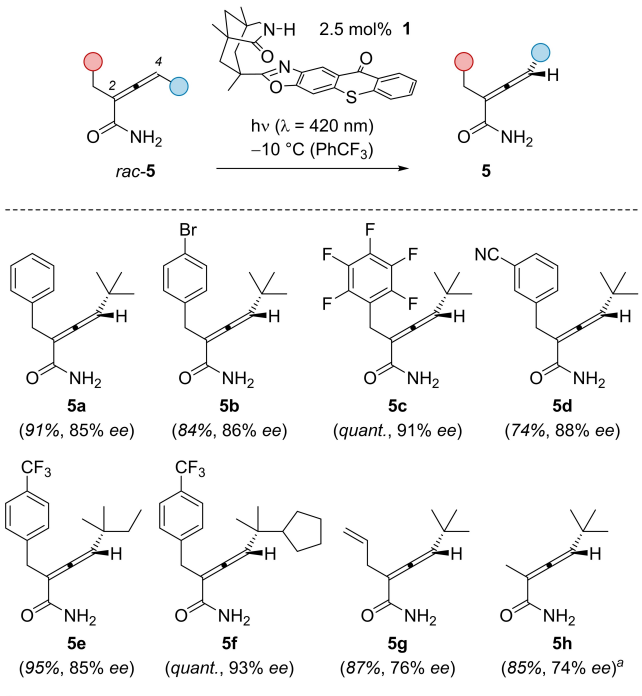

[a] Reaction performed in MeCN.

Scheme 6. Catalytic photochemical deracemization of 2,4-disubstituted 2,3-butadienamides (allene amides) *rac*-**5** mediated by chiral thioxanthone **1**: Reaction conditions and a selection of products.

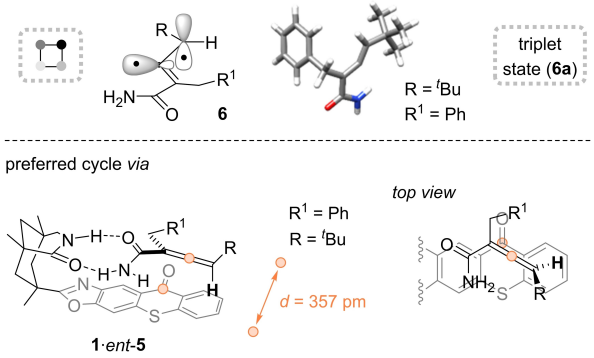

Scheme 7. Diradical **6** as a putative achiral intermediate in the deracemization of allene amides *rac*-**5** and the conformation of **6a** as obtained from conformational sampling at the GFN2-xTB level and subsequent refinement using density functional theory (DFT) calculations (top). The enantiomer *ent*-**5** is preferentially processed by catalyst **1** via complex **1**·*ent*-**5** which is conformationally locked by a CH-π interaction between the C–**H** bond at the terminal allene carbon atom and the outer benzo ring of the thioxanthone (bottom).

found computationally that enantiomer *ent*-**5** is coordinated to the catalyst not only by two hydrogen bonds but also by a significant dispersion interaction. Its terminal hydrogen atom locks the allene to the thioxanthone by a CH-π interaction and, thus, enforces a small distance to the catalyst, which was calculated for *ent*-**5a** to be only 357 pm for the indicated carbon atoms in complex **1**·*ent*-**5**.

The major enantiomer showed a similar hydrogen bonding interaction but here the *ortho*-hydrogen atoms of the aryl groups force the chromophore away from the sensitizing unit, hence increasing the distance to the thioxanthone ring. This observation nicely explained the particularly selective reaction of 2-arylmethyl substituted allenes. It was possible to determine the triplet energy for an allene amide from phosphorescence studies as $E_T = 272\ kJ\,mol^{-1}$ (77 K, EtOH). The value was further verified by sensitization experiments, in which the racemization of an allene was studied in the presence of compounds with different triplet energies. Therefore, the energy transfer from the catalyst is slightly endergonic and requires the proximity of the two chromophores. Minimum energy conical intersections (MECIs) were calculated at which the two low-lying triplet states become degenerate. A low lying MECI suggests a facile population of the triplet intermediate **6**. It was found that the MECI geometry is decidedly lower in energy for the complex $T_1(\mathbf{1})\cdot ent\text{-}\mathbf{5a}$ ($+52\ kJ\,mol^{-1}$) as compared to the diastereomeric complex $T_1(\mathbf{1})\cdot\mathbf{5a}$ ($+79\ kJ\,mol^{-1}$). The lower activation barrier accounts for a higher rate with which *ent*-**5a** is processed in the preferred catalytic cycle.

2.2. Alkenes

The double bond of alkenes does typically not constitute an element of chirality but rather accounts for the relative configuration by being either (*E*)- or (*Z*)-configured. Extensive work on the selective photochemical $E \rightarrow Z$ isomerization has been performed in recent years either by using a distinct irradiation wavelength or an appropriate triplet sensitizer.[11] Moreover, it is long known that cyclic (*E*)-alkenes exhibit planar chirality because the linker connecting the two olefinic carbon atoms cannot freely rotate. Creative experimental studies have been conceived which aimed at the enantioselective formation of chiral (*E*)-alkenes from achiral (*Z*)-alkenes. In particular, the group of Y. Inoue has made significant contributions to the field, mostly employing Förster (singlet) energy transfer.[22]

A deracemization of alkenes, according to the definition provided above, is possible if axially chiral alkenes are taken as starting materials. In this case, there is no achiral (*Z*)-alkene involved but rotation around the double bond leads to the opposite enantiomer. A frequently encountered compound class displaying axial chirality is represented by alkylidenecycloalkanes containing different substituents at the double bond and in the cycloalkane ring (Scheme 8).

By translating the developed deracemization strategy based on selective triplet energy transfer from chiral thioxanthone-based catalyst *ent*-**1**, an array of alkylidenecycloalkanes *rac*-**7**, varying in ring size ($n = 1$ or 2), were amenable to deracemization.[23] By using only 2.0 mol% of ent-**1**, enantioenriched alkenes **7** were obtained in excellent yield and high enantiomeric excess (up to 96% *ee*). In particular, the use of silicon-based functional groups in the cycloalkane backbone positively influenced the obtained optical purity of cyclobutanone-derived ($n = 1$) olefins (**7c**, **7d**). In the reaction set of alkylidenecyclopentanes ($n = 2$), not only diaryl-substituted substrates (**7e**, **7f**), but also *cis*-hydrindane **7g** were tolerated under the applied reaction conditions, resulting in high enantioselectivities. The mecha-

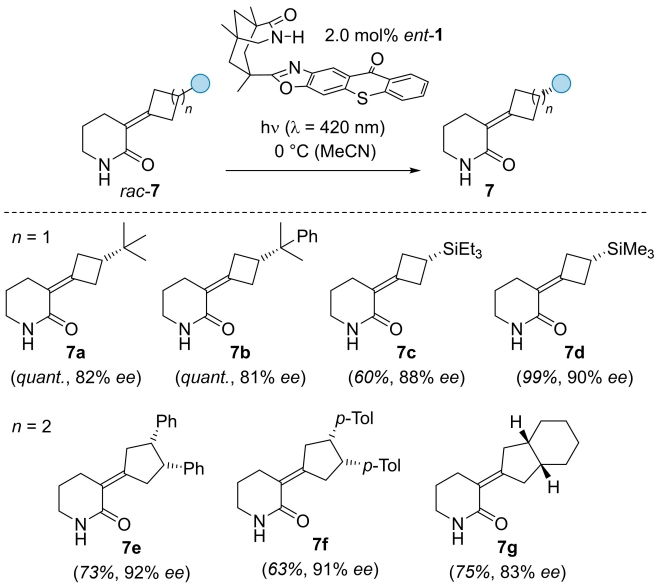

Scheme 8. Catalytic photochemical deracemization of alkylidenecyclobutanes ($n = 1$, *rac*-**7a–7d**) and alkylidenecyclopentanes ($n = 2$, *rac*-**7e–7g**) mediated by chiral thioxanthone *ent*-**1**: Reaction conditions and a selection of products [*p*-Tol = *para*-methylphenyl].

nistic analysis of the reaction follows the pattern described for allenes. The formation of complex **1**·*ent*-**7** is preferred over the formation of complex **1**· **7** as confirmed by NMR titration experiments (Scheme 9).

The rate of sensitization was assessed by computational methods focusing on the MECI geometries for the triplet energy transfer from thioxanthone to alkene. Two relevant conformers for the alkylidenecycloalkanes **7a** and *ent*-**7a** were identified which were treated in separate calculations. Comparable transition states for energy transfer were found to be lower in the case of **1**·*ent*-**7a** vs. **1**·**7a**. After energy transfer, a free rotation leads to intermediate **8** from which both enantiomers are accessed statistically.

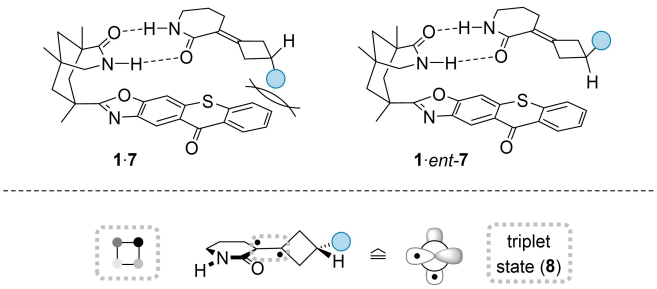

Scheme 9. Deracemization of alkylidenecycloalkanes *rac*-**7** occurs via hydrogen-bonded complexes **1**·**7** and **1**·*ent*-**7**. The latter is preferred and leads upon energy transfer to an achiral triplet intermediate **8** from which both enantiomers can be formed. The preference for processing *ent*-**7** over **7** is also in this case mainly ascribed to a faster energy transfer step.

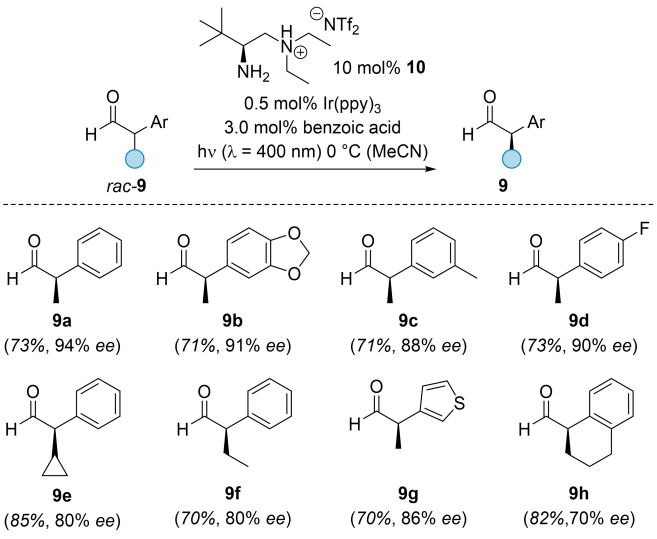

Scheme 10. Catalytic photochemical deracemization of α-arylated aldehydes *rac*-**9** mediated by a racemic iridium catalyst and chiral amine **10**: Reaction conditions and a selection of products [ppy = 2-phenylpyridine].

2.3. Enamines

Due to the ever-growing development in the field of enantioselective organocatalysis, the synthesis of *α*-branched tertiary aldehydes with a defined configuration is well established.[24] Despite significant achievements in the area, it is highly desirable in the context of atom economic synthesis to directly access enantiopure aldehydes from their racemates.

Based on previous studies on enamine protonation,[25] the group of Luo developed a procedure for the deracemization of aryl-substituted aldehydes *rac*-**9** bearing an *α*-stereogenic center.[26] While triplet energy transfer was utilized as the vehicle for the generation of the key intermediate, the method does not employ a chiral photocatalyst, but rather a multi-catalytic system, using racemic photocatalyst $Ir(ppy)_3$ as the triplet sensitizer and chiral aminocatalyst **10** (Scheme 10). A wide range of *α*-aryl aldehydes *rac*-**9**, showing various functional groups, was subjected to the deracemization conditions resulting in the corresponding enantioenriched compounds **9** in high yields and with high enantiomeric excess (up to 96% *ee*). Substrates that incorporated an aldehyde as well as a ketone moiety exclusively showed deracemization at the α-position of the aldehyde, but no reactivity at the *α*-stereogenic center of the ketone.

The high selectivity for stereogenic centers neighboring an aldehyde was successfully employed for the epimerization of substrates that displayed additional stereogenic centers with defined configuration, which were not affected by the deracemization protocol. A limitation of the method is the incompatibility with substrates that do not possess an aryl group in the α-position or lack an aldehyde moiety, such as *α*-aryl ketones.

Enamines would not, *per se*, be considered short-lived intermediates as defined in the introduction. However, in the present case the key feature of the deracemization is the formation of the thermodynamically disfavored (*Z*)-isomer (*Z*)-**11** from diastereoisomer (*E*)-**11**. This isomer is not accessible by a ground state process and plays, according to the authors, a pivotal role in the deracemization reaction (Scheme 11). In line with reported data on (*E*)- vs. (*Z*)-configured stilbenes,[27] the triplet energy of the (*E*)-**11** isomer was assumed to be lower than that of (*Z*)-**11**. Calculated values (DFT) for the vertical transition $S_0 \rightarrow T_1$ were found to be 301 kJ mol^{-1} for (*E*)-**11** and 313 kJ mol^{-1} for (*Z*)-**11**. The triplet energy of the iridium catalyst $Ir(ppy)_3$ had been determined experimentally as $E_T = 235$ kJ mol^{-1} (77 K, CH_2Cl_2).[28] While this value suggests triplet energy transfer to be impossible for neither (*E*)-**11** nor (*Z*)-**11**, the real E_T values are likely lower than the vertical excitation energies and the triplet energy of (*E*)-**11** is in a range that allows for sensitization. Two other factors are postulated to be relevant for the enrichment of enantiomer **9** in the deracemization reaction. The enantiomer reacts more slowly than *ent*-**9** with amine **10** to form enamine (*E*)-**11** and protonation of enamine diastereoisomer (*Z*)-**11** occurs preferentially to form product **9** but not its enantiomer. The key intermediate responsible for the interconversion of (*E*)-

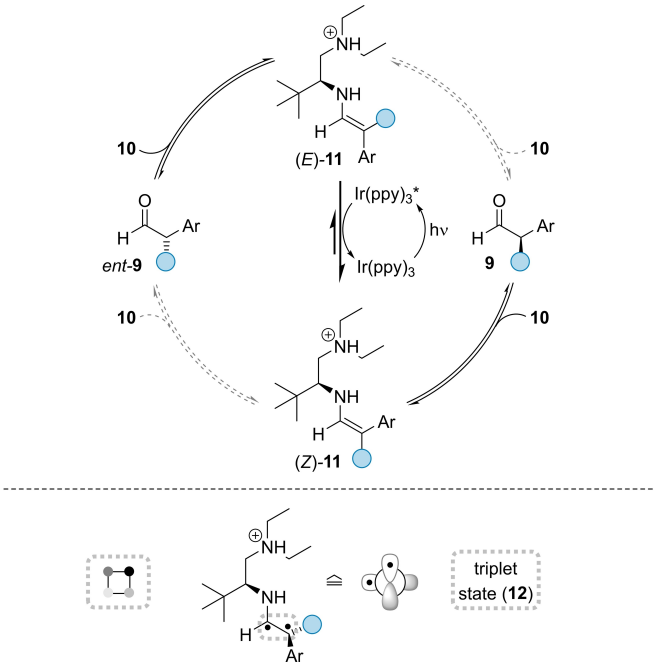

Scheme 11. Enamine protonation of diastereoisomer (*Z*)-**11** occurs selectively from one diastereotopic face to provide aldehyde **9**. The iridium catalyst ensures population of this isomer via selective energy transfer to the (*E*)-isomer (*E*)-**11**. Formation of enamine (*E*)-**11** from aldehyde enantiomer *ent*-**9** is rapid, which increases the overall preference for deracemization in favor of product **9**. Selective *E*→*Z* isomerization occurs via triplet intermediate **12**.

11 to (*Z*)-**11** is the triplet state **12** which was calculated to be 227 kJ mol^{-1} above ground state.

3. Cleavage of C–H Bonds

Ubiquitous in both nature and pharmacologically active compounds,[29] sp^3-hybridized tertiary carbon centers represent an attractive, arguably the most attractive target for photochemical deracemizations. In many cases, these substrates do not exhibit an addressable chromophore, which can be excited for the formation of an achiral intermediate in order to erase the chiral information. Therefore, suitable catalytic systems are required to generate a non-stereogenic carbon center in situ. In this section, the presented mechanisms employ three types of achiral intermediates which can be categorized into *C*-centered radicals, enols, and enolates.

3.1. Imidazolidinones

The use of photoredox catalysis[30] offers an efficient way of generating the necessary achiral intermediate for deracemization reactions by a stepwise ablation of the stereogenic information at an sp^3-hybridzed carbon atom. Knowles,Miller and co-workers disclosed the deracemization of imidazolidinones *rac*-**13** based on the use of a photoredox catalyst, a chiral phosphate **14**, and tetrapeptide **15** (Scheme 12).[31] In combination with triphenyl methane and molecular sieves, a variety of cyclic ureas (*rac*-**13**) were shown to undergo successful deracemization, displaying different substitution patterns at the stereogenic center (**13a**–**13c**) as well as at the urea nitrogen atoms (**13d**, **13e**). Also the use of an *N*(1)-unsubstituted imidazolidinone was tolerated under the conditions of the deracemization protocol. Moreover, the performance of this multi-catalytic system was underlined by the almost complete inversion of *ent*-**13a** to its mirror image **13a** in excellent yield.

The mechanistic picture of the imidazolidinone deracemization reveals the role of the individual components within the chosen catalytic system (Scheme 13). The iridium catalyst is required to oxidize the substrate and only 3-aryl-substituted imidazolidinones display a sufficiently low oxidation potential to allow for an electron transfer. The authors report a half-peak potential for the oxidation of compound *rac*-**13a** as $E_{ox} = +0.91$ V (vs. Fc^+/Fc, CH_3CN) and a calculated redox potential $E_{1/2}(Ir^{III*}/Ir^{II}) = +0.94$ V (vs. Fc^+/Fc, CH_3CN) for the selected iridium catalyst rendering the formation of radical cation **16** possible. At this stage, a first discrimination occurs by the chiral phosphate base **14** which preferentially deprotonates (*R*)-**16** leading to the achiral radical **17**. Although it has not been spectroscopi-

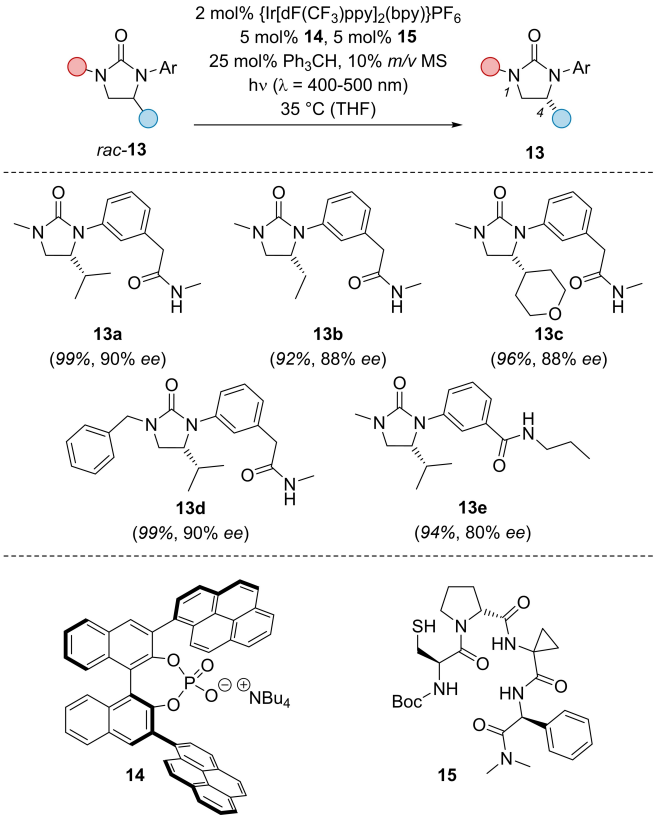

Scheme 12. Photochemical deracemization of 3-aryl-2-imidazolidinones *rac*-**13** by cooperative catalysis of an iridium catalyst, a chiral phosphate **14** and a synthetic tetrapeptide **15**: Reaction conditions and a selection of products [Boc = *tert*-butoxycarbonyl, bpy = 2,2′-bipyridine, MS = molecular sieves].

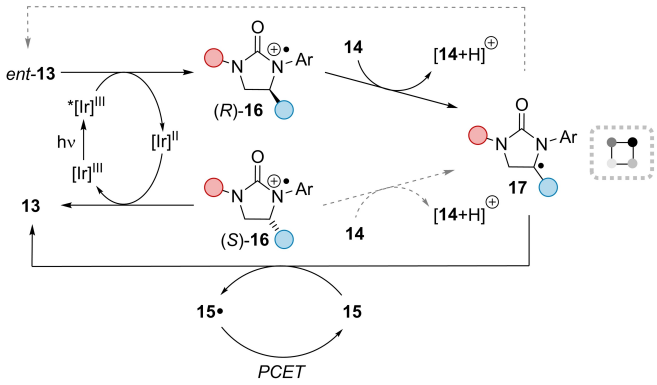

Scheme 13. Chiral catalysts in the deracemization of 3-aryl-2-imidazolidinones operate on two selectivity levels. The chiral phosphate facilitates deprotonation of radical cation (*R*)-**16** over (*S*)-**16** while the chiral tetrapeptide **15** undergoes a selective hydrogen atom transfer (HAT) to form enantiomer **13** from radical intermediate **17**.

cally detected, the intermediacy of **17** is strongly suggested by DFT calculations and by experimental data. In fact, an achiral intermediate (cf. Scheme 2) needs to be formed and it is sensible to assume that radical **17** returns to the substrate upon hydrogen atom transfer (HAT) from the cysteine-containing tetrapeptide **15**. In this step, there is a preference in favor of product **13** and the two steps, radical formation and HAT, work synergistically to preferentially afford product **13**. The cysteine radical is reduced by the Ir^{II} intermediate to regenerate thiol **15** by a proton coupled electron transfer (PCET) involving the phosphoric acid [**14**+H]$^+$. The aryl groups in position N3 of substrates *rac*-**13** ideally display a secondary amide as a hydrogen bonding handle that increases the interaction with the peptide.

The synergy of the two chiral catalyst components **14** and **15** was demonstrated by replacing either one of them with an achiral catalyst. If the chiral phosphate **14** was substituted by achiral tetrabutylammonium diphenyl phosphate, product **13a** was obtained in 58 % *ee*. If thiophenol was used instead of tetrapeptide **15** as HAT source, the enantioselectivity decreased to 72 % *ee*. Taken together, the product of the individual selectivities correlates well with the observed enantiomeric excess achieved for **13a** (Scheme 12).

3.2. Pyridylketones

Conventional methods for the creation of α-stereogenic centers at ketones either involve the enantioselective formation of a new C−C bond[32] or the enantioselective protonation of an enolate species.[33] In the latter process, if the formation of one enantiomer from a racemic mixture is desired, the achiral intermediate, e.g. a silyl enol ether, has to be synthesized separately prior to being subjected to an enantioselective protonation. Meggers, Chen and co-workers overcame this two-step sequence by the photochemical formation of an enol/enolate intermediate followed by protonation.[34] They established a one-pot procedure for the deracemization of pyridylketones *rac*-**18** that makes use of a previously reported[35] chiral-at-metal rhodium photocatalyst **19** in combination with *N*-phenylpiperidine (**20**) under visible light irradiation (Scheme 14). An array of different racemic pyridylketones *rac*-**18** was subjected to the reaction conditions, furnishing the optically active products **18** in generally high yields and high enantioselectivities. Apart from different functional groups at the α-aryl moiety or the pyridine ring (**18a**–**18c**, **18f**), the use of different substitution patterns at the stereogenic center was demonstrated to be compatible with the deracemization, including the use of α-amino ketones (**18d**) or the exchange of the α-methyl group for a fluorine atom (**18e**). In order to highlight the synthetic utility of this method, **18a** was successfully converted in a set of follow-up transformations to a range of downstream products with almost complete retention of configuration. Consecutive reactions included the formation of the corresponding alkyl pyridine by stepwise carbonyl reduction or of picolinates by a Baeyer–Villiger oxidation.

The ketone deracemization is proposed to be initiated by an oxidation of amine **20** by the photoexcited rhodium complex **21** (Scheme 15). From CV data and its triplet state energy, its redox potential was calculated as $E_{1/2}$(**21**$^{*+}$/**22**$^{\bullet}$) ≅ +1.6 V (vs. Ag/AgCl, CH_2Cl_2) which is sufficiently high to oxidize an amine. Complex **21** was found to display an increased absorbance in the emission regime of the chosen light source as compared to acetonitrile complex **19**. The chiral enolate **23** is formed by HAT of the α-hydrogen atom from radical **22** to the amine radical cation. The subsequent

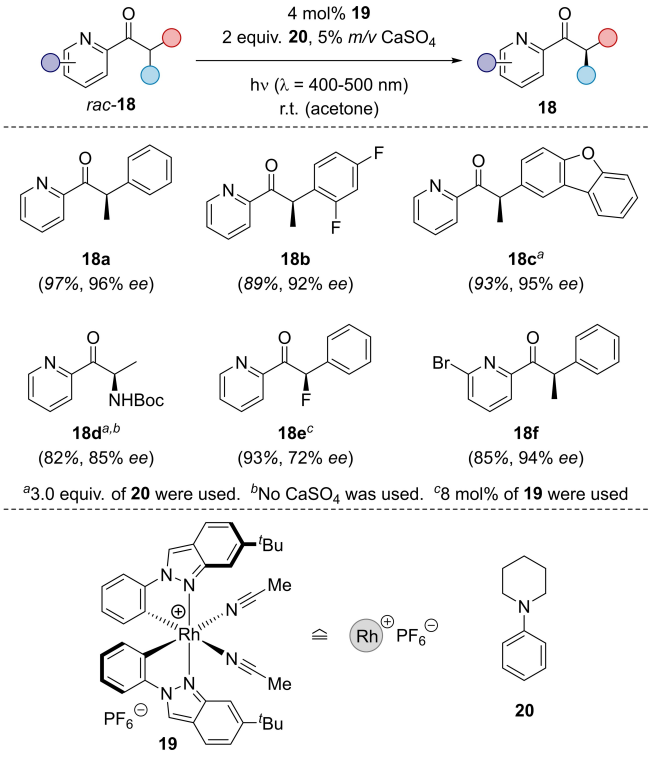

Scheme 14. Catalytic photochemical deracemization of α-chiral 2-pyridylketones *rac*-**18** mediated by chiral Lewis acid **19** and achiral amine **20**: Reaction conditions and a selection of products.

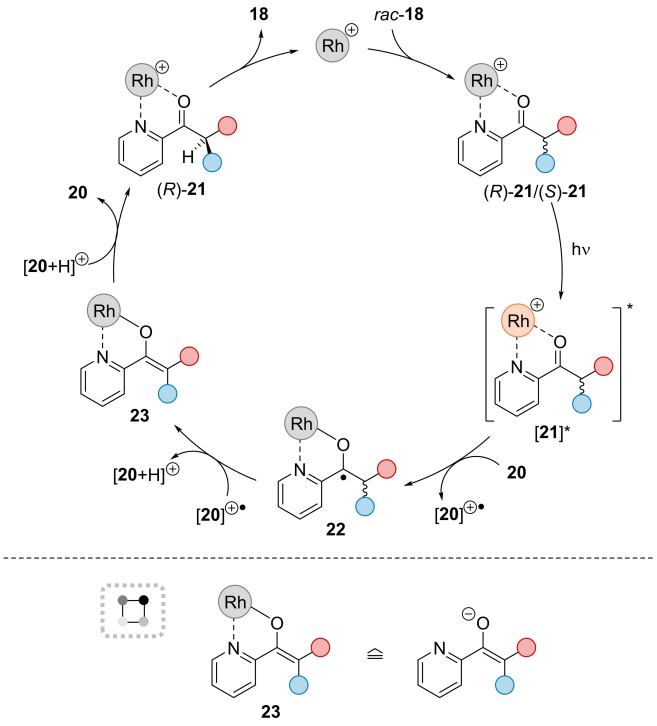

Scheme 15. Postulated mechanism for the deracemization of α-chiral 2-pyridylketones *rac*-**18**: The formation of enolate **23** does not occur by deprotonation but by consecutive electron/hydrogen atom transfer steps. Both enantiomers of ketones *rac*-**18** are processed and the formation of product **18** is the result of a preferred protonation **23**→(*R*)-**21**.

protonation of enolate **23** is rendered diastereoselective by the chirality at the metal center delivering the rhodium-bound ketone with (*R*)-configuration. If the rhodium complex **23** was formed quantitatively by a deprotonation reaction and protonated, the enantioselectivity of **18** was lower (50 % *ee*) than in the deracemization reaction. Based on computational studies, the authors suggest that complex (*S*)-**21** is formed from *rac*-**18** and **19** preferentially over (*R*)-**21** which explains the high selectivity and the absence of substrate inhibition. If α-deuterated substrate *rac*-**18** was taken into the deracemization reaction, 40 % of product **18** remained deuterated. While the authors take this observation as evidence that the amine cation $[\mathbf{20}+\mathrm{D}]^+$ or residual water serve as sources for deuterium or hydrogen, it could indicate that this product fraction was not processed at all, which is in line with the hypothesis that complex (*S*)-**21** is formed and processed more efficiently than (*R*)-**21**.

3.3. Hydantoins

Due to their prominence in pharmaceuticals and their direct synthetic and structural relation to α-amino acids,[36] hydantoins (*rac*-**24**) represent valuable targets for enantioselective synthesis. They exhibit a lactam binding motif which appeared to enable binding to azabicyclo[3.3.1]nonanones (as seen in catalyst **1**) by two-point hydrogen bonding. It was hypothesized that a reversible HAT was feasible at the stereogenic center if an appropriate chromophore was placed at the tricyclic lactam backbone. Based on previous work on enantioselective, photoinduced electron transfer,[37] benzophenone **25** was chosen as the chiral photocatalyst since the benzophenone moiety is well-known for its capability to abstract hydrogen atoms. Preliminary calculations indicated that one hydantoin enantiomer would display its hydrogen atom in close proximity to the carbonyl group of the benzophenone. It was therefore anticipated that—as in the case of triplet energy transfer—one enantiomer would be favorably processed. However, it was also seen in preliminary work with achiral, parent benzophenone that HAT can lead to a suite of side reactions. Still, the deracemization reaction was attempted and proceeded remarkably well. Side reactions were not detectable and yields of enantioenriched products were high, frequently higher than 80 %. A set of structurally different hydantoins *rac*-**24** was successfully deracemized by using only 5 mol% benzophenone **25** in trifluorotoluene as the solvent, resulting in nearly enantiopure products **24** (Scheme 16).[38] In order to allow for a successful deracemization, *N*-phenyl substitution turned out to be crucial, whereas a wide range of sterically different alkyl groups (**24a**–**24c**) as well as functional group-containing alkyl and aryl moieties (**24d**–**24g**) at the stereogenic center were tolerated.

While the forward HAT in the deracemization of hydantoins seemed straightforward and accounted for the preferential formation of enantiomers **24** with (*R*)-configuration, it was unclear how the hydrogen atom was returned from the protonated ketyl radical to the putative hydantoin radical. Deuterium labelling experiments suggested this process to occur statistically. For example, if a mixture of two different (*S*)-hydantoins, with one of them completely deuterated and the other non-deuterated, was subjected to complete inversion with catalyst **25**, the obtained (*R*)-

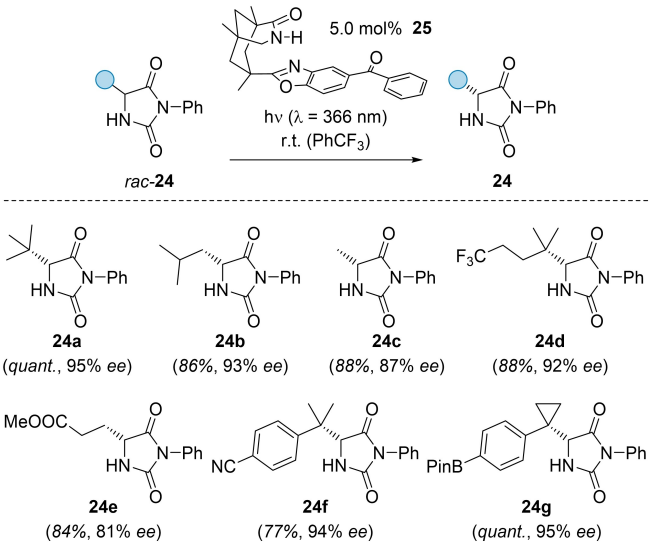

Scheme 16. Catalytic photochemical deracemization of imidazolidine-2,4-diones (hydantoins) *rac*-**24** mediated by chiral benzophenone **25**: Reaction conditions and a selection of products [Pin = pinacolate].

hydantoins both contained ca. 50 % deuterium. In order to study this phenomenon more closely, the reaction was investigated by computational methods, association experiments, and transient absorption spectroscopy. For supply reasons, the mechanistic experiments were performed with *ent*-**25**, the enantiomer of catalyst **25**.[38b] Catalyst *ent*-**25** delivered (*S*)-hydantoins *ent*-**24** as major products, therefore preferentially abstracting a hydrogen atom from (*R*)-enantiomer **24** (Scheme 17). NMR titration experiments showed a slightly higher binding constant for **24** as compared to *ent*-**24**. Transient absorption spectroscopy studies with *ent*-**25** in the presence of either one of the two enantiomers corroborated the hypothesis that only one enantiomer, in this case enantiomer **24**, undergoes HAT to the benzophenone, thus, forming protonated ketyl radical *ent*-**26** and hydantoin radical **27**. The lifetime of *ent*-**26** could be measured as τ = 181 ns and indicated that back HAT occurs rapidly. The process was monitored for substrate *rac*-**24a** by computational methods. Complex *ent*-**25**·**24a** was structurally optimized and it was found that upon excitation and intersystem crossing (ISC) the HAT within *ent*-**25***·**24a** occurs with a low activation barrier of only 57 kJ mol^{-1}. Intriguingly, a transient hydrogen bond between the hydrogen atom of the protonated ketyl radical *ent*-**26** and the carbonyl group of **27** further stabilizes the intermediate complex *ent*-**26**·**27**, preventing the diffusion of free radicals in solution and the formation of radical-coupling products. Moreover, the hydrogen bond suitably positions the hydrogen atom of protonated ketyl radical *ent*-**26** and carbon-centered hydantoin radical **27** for subsequent back HAT. Hence, upon ISC to the singlet hypersurface, the carbonyl oxygen atom adjacent to the prostereogenic carbon atom of **27** receives the hydrogen atom generating achiral enol tautomer **28**. The latter intermediate was detected by transient absorption spectroscopy and displayed a lifetime of τ = 2 µs. Following the dissociation of complex *ent*-**25***·**28**, enol **28** subsequently tautomerizes unselectively to either enantiomer *ent*-**24** and **24**. Due to the large barrier of the HAT step to become kinetically relevant in complex *ent*-**25**·*ent*-**24**, *ent*-**24** is not further processed by the catalyst and, hence is enriched over several catalytic cycles.

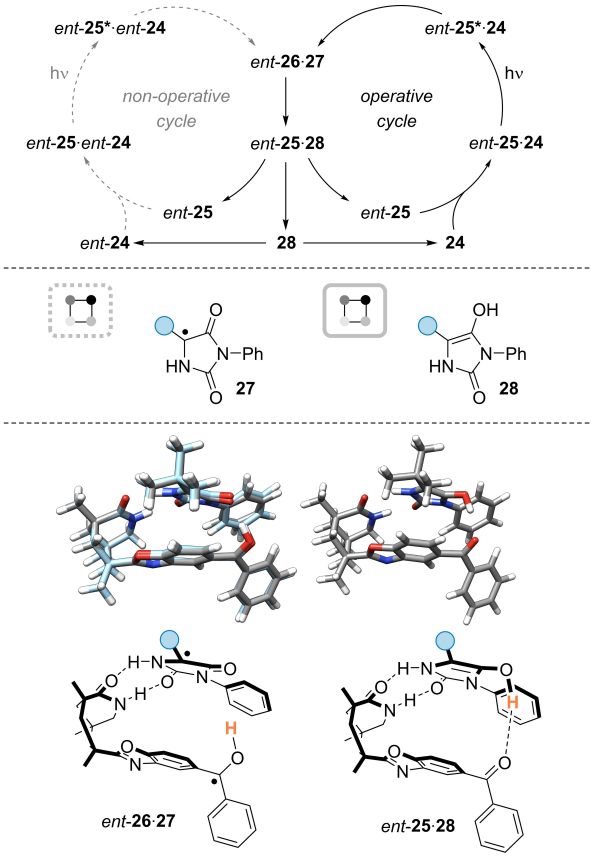

Scheme 17. Deracemization of hydantoins as studied for catalyst enantiomer *ent*-**25** leading to (*S*)-configured products *ent*-**24**: Hydrogen abstraction occurs rapidly in complex *ent*-**25***·**24** generating protonated ketyl radical *ent*-**26** and hydantoin **27** which remain attached by hydrogen bonds. Back HAT occurs to the oxygen atom forming enol **28** from which the two enantiomers form statistically. Since only enantiomer **24** is processed, the other enantiomer represents the only/major product.

3.4. α-Amino Acid Esters

Based on their fundamental role as building blocks in peptides and due to their ubiquity in various bioactive molecules, the synthesis of enantiopure natural α-amino acids is a long-standing benchmark for enantioselective method development. In a recent study, the group of Jiang developed a deracemization protocol that furnishes enantioenriched *N*-arylated α-amino acid esters **29** and related compounds. They used organic photocatalyst **30** in combination with a chiral Brønsted acid **31** (Scheme 18) employing two major procedures A and B.[39] Upon variation of the optimized reaction conditions for some substrates, overall high yields and enantioselectivities were observed. Apart from different aryl and alkyl moieties at the stereogenic center (**29a**–**29d**), electron-rich functional groups within the *N*-aryl group (**29e**) as well as different esters (**29f**) and pipecolic acid derivatives (**29g**) were compatible with the deracemization protocol. It was further possible to address the stereogenic center of α-amino lactones, ketones and α-diaryl-substituted secondary amines. Moreover, a selective editing of the stereogenic center in α-position to the amino group was demonstrated by subjecting complex scaffolds containing several defined stereogenic centers to the reaction conditions.

The presence of an *N*-aryl group in all substrates *rac*-**29** already suggests this entity to be crucial for the deracemization process (Scheme 19). It was proposed that the photocatalyst oxidizes the amino group in its excited state **30***. Given that the reported calculated redox potential of intermediate **30*** is $E_{1/2}(\mathbf{30}^*/\mathbf{30}^{\bullet-}) = +1.42$ V (vs. SCE, CH_3CN) and the oxidation potential of the *N*-arylated amino esters, e.g. for *rac*-**29a** is E_{ox} (*rac*-**29a**$^{\bullet+}$/*rac*-**29a**) = + 0.85 V (vs. SCE, CH_3CN), the process is thermodynamically feasible. Deprotonation at the stereogenic center leads to achiral radical intermediate **32** and to the protonated catalyst radical. Based on DFT calculations, the event likely

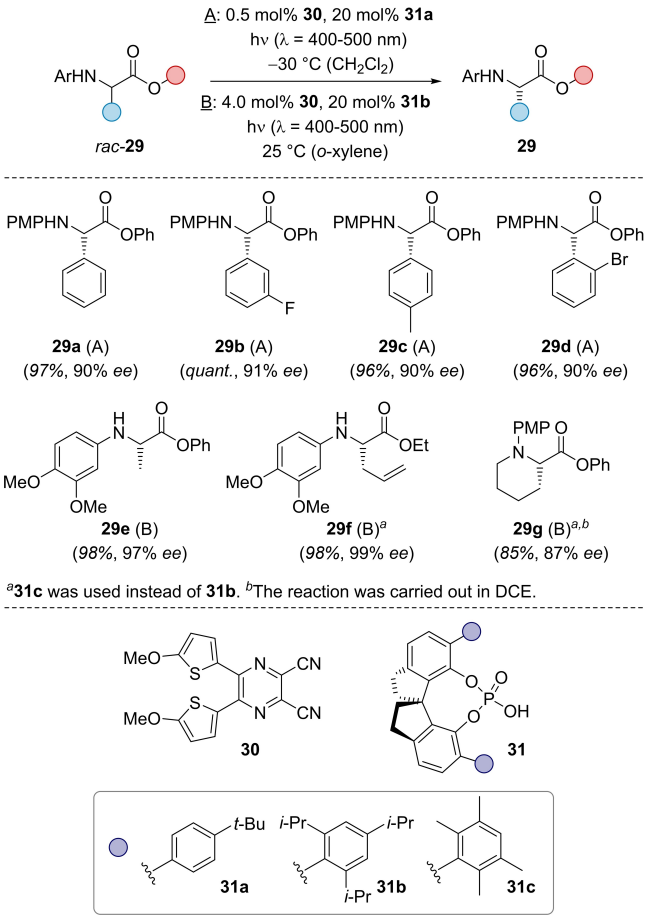

Scheme 18. Catalytic photochemical deracemization of *N*-aryl-substituted α-amino acid esters *rac*-**29** mediated by an achiral photocatalyst **30** and chiral phosphoric acids **31**: Reaction conditions and a selection of products [PMP = *para*-methoxyphenyl].

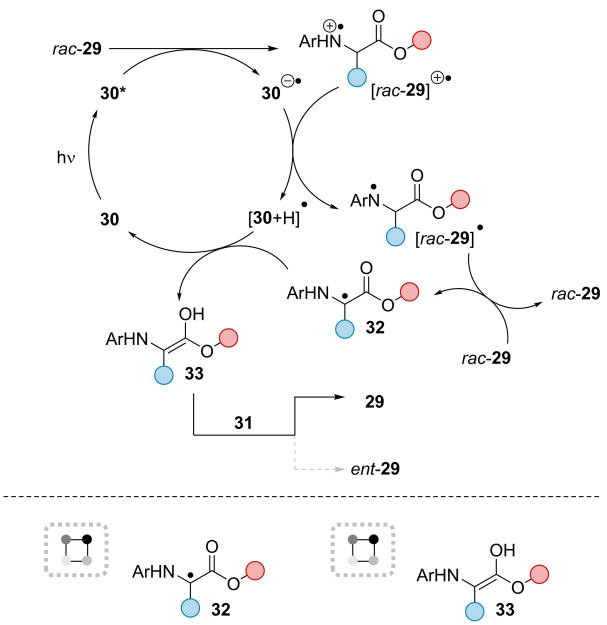

Scheme 19. The deracemization of amino esters *rac*-**29** is initiated by oxidation with photoexcited catalyst **30*** and subsequent hydrogen abstraction. Enol protonation occurs enantioselectively leading preferentially to products **29**.

occurs in a multi-step sequence that involves a second substrate molecule as a hydrogen atom shuttle. The protonated catalyst radical undergoes proton-coupled electron transfer to radical **32** generating enol intermediate **33**. The pivotal enantioselectivity-determining step (cf. Scheme 2) is the mutual proton transfer in a relatively stable complex between the enol and the respective phosphoric acid **31**. In this step, the two enantiotopic faces of the enol are differentiated with a high preference in favor of product **29**.

3.5. Oxindoles

Based on their potential as heterocyclic building blocks in biologically active compounds, the enantioselective synthesis of oxindoles has received considerable interest.[40] Despite the fact that a number of strategies exist to access 3,3-disubstituted oxindoles with defined absolute configuration, the enantioselective synthesis of 3-monosubstituted oxindoles has been hampered by their configurational lability under a variety of reaction conditions. The inherently mild reaction conditions under which photochemical deracemizations proceed allow for editing stereogenic centers prone to racemization. Therefore, it seemed promising to apply a deracemization protocol to oxindoles following a mode of action used for the deracemization of hydantoins (see chapter 3.3.). Despite oxindoles not bearing a second carbonyl group to accept a hydrogen atom, it was found that a range of 3-monosubstituted oxindoles *rac*-**34** were successfully deracemized using chiral benzophenone-based photocatalyst *ent*-**25** under irradiation with near-UV light, (Scheme 20).[41] Generally, high yields and enantioselectivities were recorded for the products **34** and various substituents were tolerated, including functionalized aryl moieties (**34a–34c**) and sterically different alkyl groups (**34d–34g**). Although with slightly diminished enantioselectivity, a substitution at the oxindole arene core was possible (**34g**, **34h**). To underline the synthetic utility of the deracemization method, the obtained oxindoles with defined configuration were used as intermediates for further transformations such as carbonyl reductions or arene hydrogenations. This enabled an access to several valuable compound classes with complete retention of configuration and the introduction of newly formed stereogenic centers with high diastereoselectivity.

Preliminary mechanistic studies involving deuterium scrambling experiments support a mechanistic scenario that is similar to the deracemization of hydantoins *rac*-**24**, with only the matched enantiomer *ent*-**34** being processed by the chiral benzophenone catalyst *ent*-**25** (Scheme 21). It was seen for the hydantoins that the back HAT from the protonated ketyl radical occurred at the oxygen atom that was not involved in hydrogen bonding. However, it appeared that if hydrogen bonding to catalysts like *ent*-**25** is sufficiently weak, atoms involved in bonding can intercept a

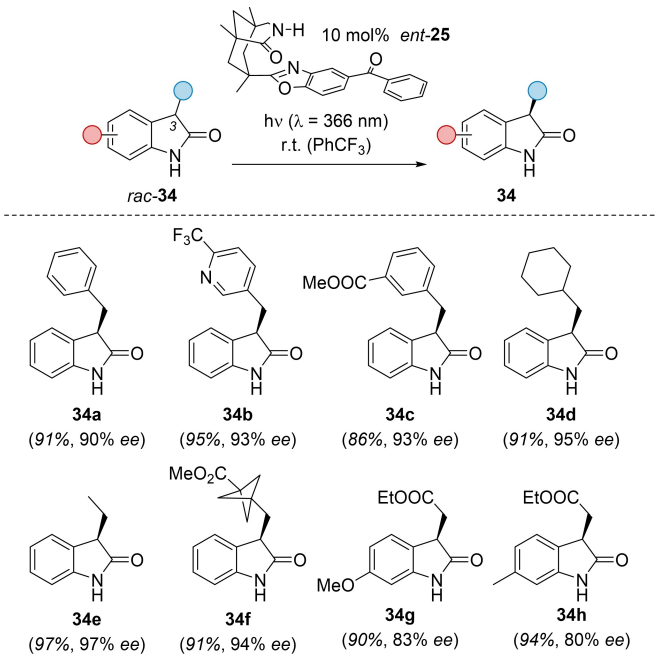

Scheme 20. Catalytic photochemical deracemization of 3-substituted 2-indolones (oxindoles) *rac*-**34** mediated by chiral benzophenone *ent*-**25**: Reaction conditions and a selection of products.

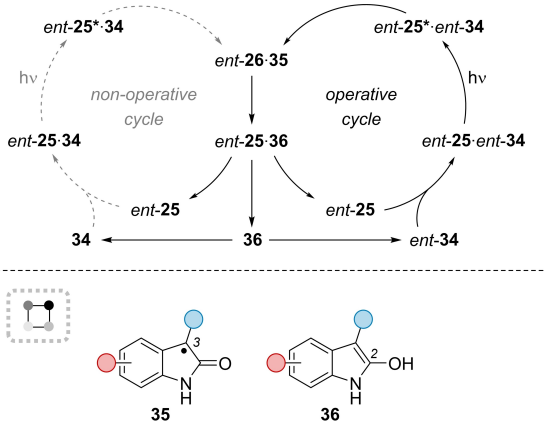

Scheme 21. The mechanistic proposal for the deracemization of 3-substituted oxindoles *rac*-**34** follows the scenario delineated for hydantoins in Scheme 17. A major difference, however, is the fact that the oxygen atom at the oxindole C2 position in radical **35** receives the hydrogen atom from the protonated ketyl radical *ent*-**26**, although involved in hydrogen bonding to the catalyst.

hydrogen atom. For oxindoles, it is necessary for the hydrogen atom of protonated ketyl radical *ent*-**26** (Scheme 17) to be returned to the oxygen atom of the hydrogen-bonded lactam radical **35** in order to ensure successful deracemization. This process would result in the transient formation of achiral 2-hydroxyindole **36**, which is anticipated to undergo statistical tautomerization to afford oxindoles *ent*-**34** and **34**. By exclusively abstracting the C3-hydrogen atom from enantiomer *ent*-**34** and transferring it into achiral intermediate **36**, an enrichment of **34** can be observed as the reaction progresses. Although the observed deuterium scrambling supports this pathway, the existence of intermediates **35** and **36** has not yet been spectroscopically substantiated. If generally applicable, the option of back HAT to an atom involved in binding significantly widens the scope of deracemization reactions based on chiral benzophenone chromophores.

4. Cleavage of other Single Bonds

The reversible cleavage of single bonds to a stereogenic carbon atom can lead to a deracemization reaction. Early work by Hammond[42] and by Ouannès[43] focused on the enantioselective formation of *trans*-1,2-diphenylcyclopropane from achiral *cis*-1,2-diphenylcyclopropane. While the reaction is not strictly a deracemization, it showed that cyclopropanes undergo a reversible ring opening upon energy transfer and that this ring opening could be a possible handle for deracemization reactions.

4.1. Cyclopropanes

The first deracemization of a cyclopropane that occurred with notable enantioselectivity (up to 55 % *ee*) was discovered in 2019.[44] In studies directed towards an enantioselective di-π-methane rearrangement of 3-allylquinolones, it was found that the resulting 3-cyclopropyl-substituted quinolones were configurationally labile when irradiated at λ = 420 nm in the presence of achiral 9-thioxanthenone. Deracemization with chiral thioxanthone *ent*-**1** was successful and triplet energy transfer was identified as the likely mode of action. Triplet energies for the quinolones were found to be in the range of $E_T = 270\ kJ\,mol^{-1}$ (77 K, $PhCF_3$). Since the first reaction step, the di-π-methane rearrangement, was also catalyzed by catalyst *ent*-**1**, most enantiomerically enriched 3-cyclopropyl-substiuted quinolones were obtained from 3-allylquinolones in a single operation (nine examples, 88–96 % yield, 32–55 % *ee*).

The result spurred interest in other cyclopropanes as deracemization substrates and spirocyclopropyl oxindoles were more closely investigated. Optimization experiments were performed with 2,2-dichlorospiro[cyclopropane-1,3′-indoline]-2′-one (*rac*-**37a**) and chiral triplet sensitizer **1**. It was found that an enantiomeric excess of up to 85 % *ee* could be achieved under irradiation with visible light employing trifluorotoluene as the solvent.[45] The 2,2-dichloro substitution at the cyclopropane ring proved to be crucial for a successful deracemization using the thioxanthone-based photocatalyst **1**, whereas various functional groups exhibiting different electronic properties at the arene were found to be compatible with the optimized reaction conditions (Scheme 22).

Mechanistic investigations were performed with parent substrate *rac*-**37a**. Despite oxindole *rac*-**37a** having a higher triplet energy ($E_T = 298\ kJ\,mol^{-1}$, 77 K, EtOH) compared to **1**, racemization studies employing achiral thioxanthone ($E_T = 274\ kJ\,mol^{-1}$, 77 K, isopentane:methylcyclohexane)[17]

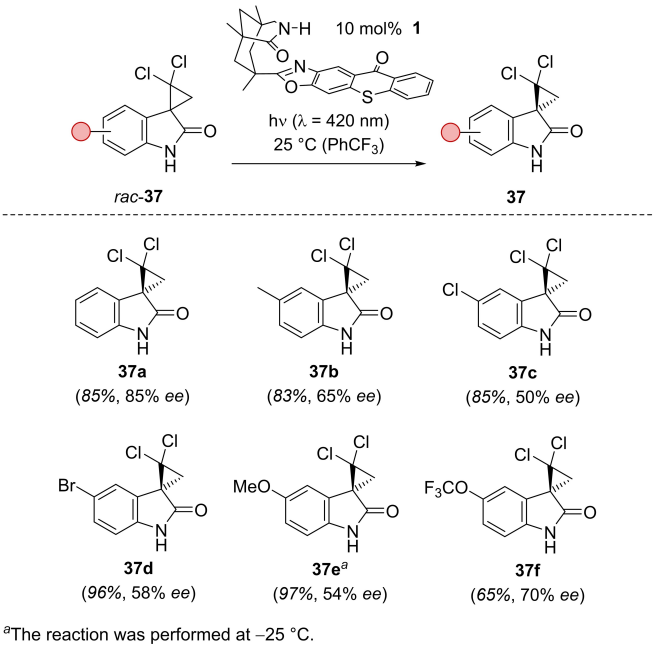

[a]The reaction was performed at −25 °C.

Scheme 22. Catalytic photochemical deracemization of 2,2-dichlorospiro[cyclopropane-1,3′-indoline]-2′-ones *rac*-**37** mediated by chiral thioxanthone **1**: Reaction conditions and a selection of products.

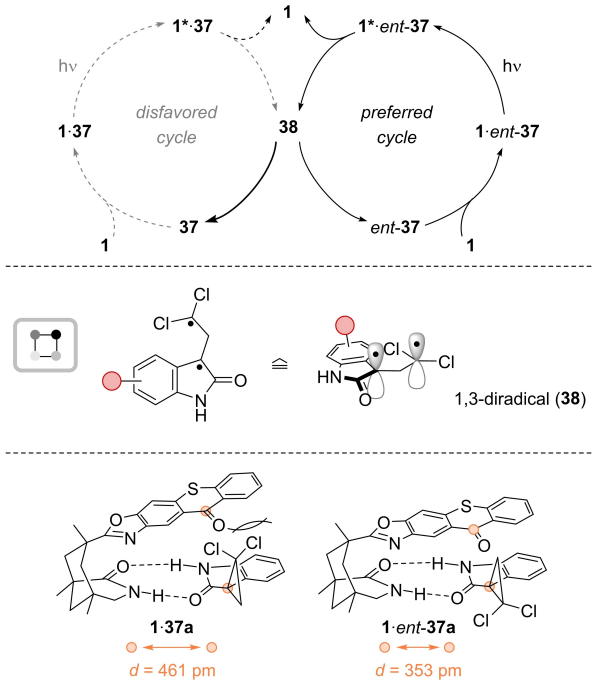

Scheme 23. The deracemization of 2,2-dichlorospiro[cyclopropane-1,3′-indoline]-2′-ones *rac*-**37** is assumed to rely on a preferential energy transfer to substrate enantiomer *ent*-**37** as compared to enantiomer **37**. The higher binding affinity of the former enantiomer to the catalyst and the decreased distance between the chromophores in complex **1**·*ent*-**37** are made responsible for the observed preference. 1,3-Diradical **38** which was spectroscopically detected is the achiral intermediate that enables the required racemization.

suggested that a triplet energy transfer is in principle possible, and that the deracemization takes place on the triplet hypersurface. For the first time, the achiral intermediate of a deracemization, in this case 1,3-diradical **38**, was detected by transient absorption spectroscopy with a lifetime of $\tau = 22$ µs in acetonitrile (Scheme 23). The specific binding constants for the two enantiomers *ent*-**37a** and **37a** to thioxanthone **1** were determined by NMR titration. Despite a preferred binding of the matched enantiomer *ent*-**37a** to the catalyst ($K_a = 250\ M^{-1}$ in benzene-d_6) in contrast to the less favored, mismatched enantiomer **37a** ($K_a = 93\ M^{-1}$ in benzene-d_6), the difference in binding preference values was unexpectedly low and did not account for the observed enantioselectivity. DFT calculations optimizing the geometry of the intermediate substrate/catalyst complexes revealed a significant difference of more than 100 pm in the distance of the chromophores in the two diastereomeric complexes **1**·**37a** and **1**·*ent*-**37a**. Rooted in the distance dependence of triplet energy transfer ($e^{-\beta\Delta d}$; $\beta = 2/L$; L: effective Bohr radius), a decrease of at least a factor of 0.37 was estimated in sensitization rate for **37a** in comparison to *ent*-**37a**. Given that L is for related chromophore couples closer to 100 pm than to 200 pm,[46] the value is likely to be even lower. This difference in triplet energy transfer in combination with the observed binding preference for *ent*-**37a** accounts for the observed enantiomeric excess in the photostationary state, with the catalytic cycle following a similar pathway as described for the deracemization of allenes (see above). 1,3-Diradical **38a** represents the achiral intermediate that leads to formation of enantiomers *ent*-**37a** and **37a** once ISC to the singlet hypersurface has occurred.

Attempts to deracemize spiro[cyclopropane-1,3′-indoline]-2′-ones *rac*-**39** displaying alkyl substituents at the cyclopropyl ring instead of a 2,2-dichloro substitution remained unsuccessful with thioxanthone-based sensitizer **1**. Further, it was found that enantiopure oxindoles **39** did not racemize upon irradiation in the presence of achiral 9-thioxanthenone ($\lambda = 420$ nm). The results indicated that their triplet energy was too high to be amenable for energy transfer from thioxanthone **1**. However, the deracemization of oxindoles *rac*-**39** became possible upon using chiral xanthone-based catalyst **40**, exhibiting a significantly higher triplet energy ($E_T = 316\ kJ\ mol^{-1}$, 77 K, pentane/isopentane).[47] By the selection of an appropriate reaction temperature (room temperature or −25 °C), enantioselectivities of up to 82 % *ee* were possible for a set of differently substituted spirocyclic oxindoles **39** (Scheme 24). Mechanistically, the reaction was believed to occur in analogy to the deracemization of cyclopropanes *rac*-**37** with xanthone **40** being responsible for processing enantiomer *ent*-**39** preferably over enantiomer **39**.

As elaborated in the introduction (cf. Scheme 2), a photochemical deracemization can also be achieved by an enantioselective reaction of a short-lived, photochemically generated intermediate. Along these lines, the group of Gilmour has explored another way of accessing enantioenriched cyclopropanes from their racemic mixture.[48] They successfully employed a chiral aluminum-salen photoredox

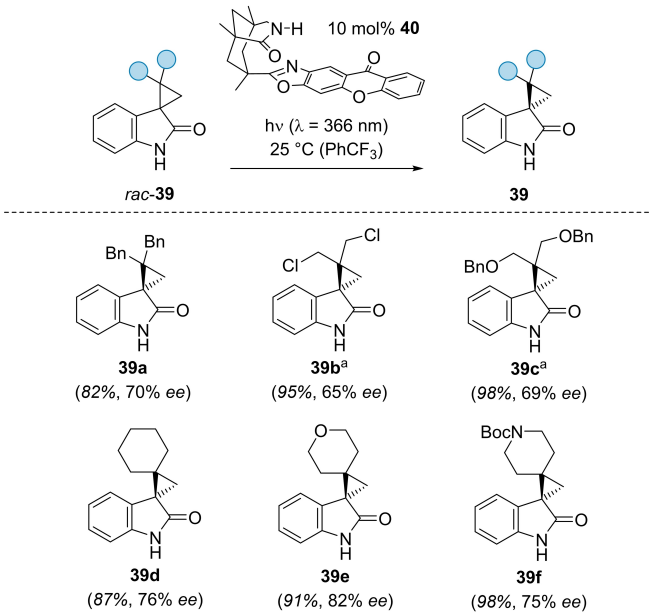

[a]Reactions were performed at −25 °C.

Scheme 24. Catalytic photochemical deracemization of 2,2-dialkyl-substituted spiro[cyclopropane-1,3′-indoline]-2′-ones *rac*-**37** mediated by chiral xanthone **40**: Reaction conditions and a selection of products [Bn = benzyl].

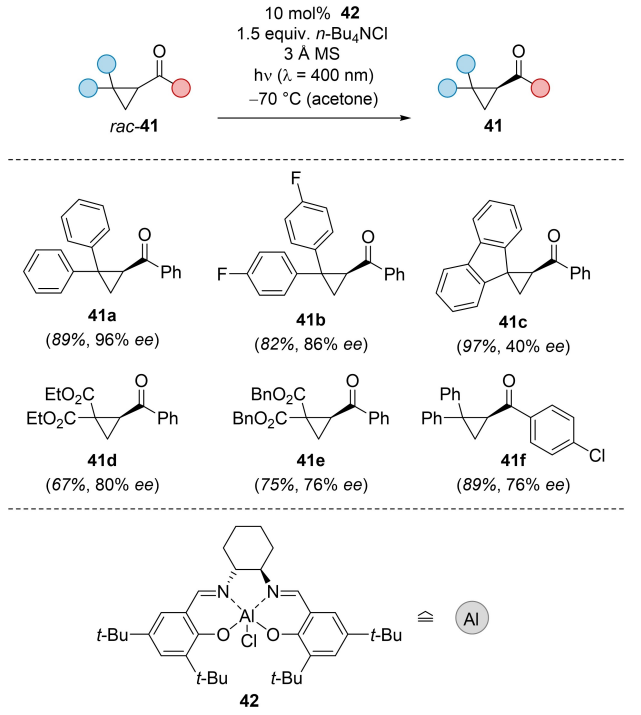

Scheme 25. Catalytic photochemical deracemization of cyclopropylketones *rac*-**41** mediated by chiral Lewis acid **42**: Reaction conditions and a selection of products.

catalyst **42** for the deracemization of cyclopropyl ketones *rac*-**41**, furnishing the desired products with generally high yields and enantioselectivities of up to 96 % *ee* (Scheme 25). The addition of *n*-Bu_4NCl was required for constant high yields and enantioselectivities. Apart from different symmetric *gem*-substitutions at the cyclopropyl moiety (**41a**–**41e**), variations of the aryl ketone (**41f**) were also well-tolerated. By using unsymmetrically substituted cyclopropyl ketones, a formal kinetic resolution was initiated under the irradiation conditions, leading to the two enantiomerically enriched diastereoisomers with medium to high enantioselectivities but without profound diastereoselectivity. This applies to reactions where only one racemic diastereoisomer was irradiated as well as for irradiation experiments with racemic mixtures of the *cis*- and *trans*-substituted cyclopropyl ketones.

The mechanistic picture provided by Gilmour and coworkers for the deracemization of cyclopropyl ketones rests on the binding of aluminum complex **42** to the ketone by a Lewis acid/base interaction (Scheme 26). They propose that both enantiomers form a complex, depicted here as (*S*)-**43** and (*R*)-**43**, which are excited by visible light (λ = 400 nm). Time-dependent DFT calculations indicated that the excited complex **43*** displays significant charge transfer character due to electron transfer from the ligand to the carbonyl group of the ketone. As a result, aluminum-bond ketyl radical **44** was postulated. Due to the unpaired electron residing in the π*-orbital of the carbonyl group, a bond fission of the adjacent single bond is induced. The ring opening erases the stereogenic center at the cyclopropane ring and generates a radical connected to chiral aluminum

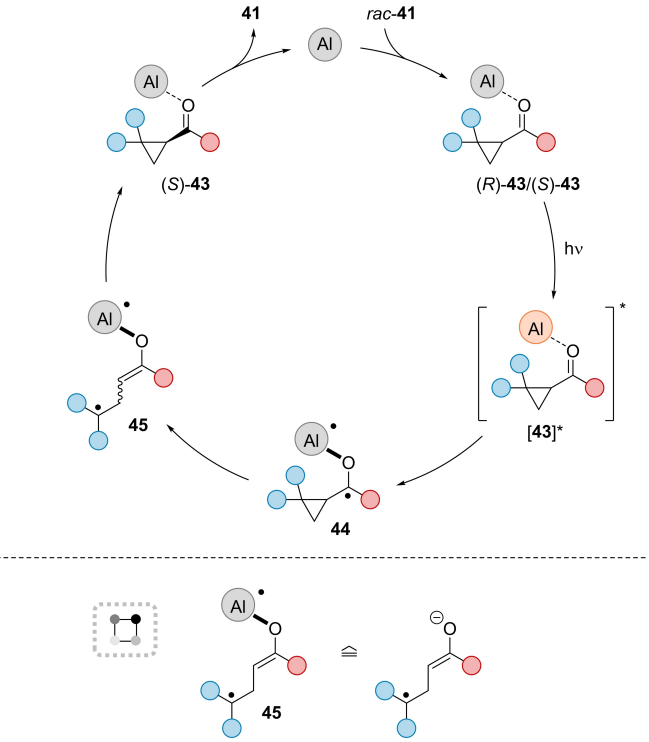

Scheme 26. Deracemization of cyclopropanes *rac*-**41** mediated by chiral aluminum-salen complex **42**. An enantioface differentiation in the cyclization step **45**→(*S*)-**43** accounts for the observed enantioselectivity.

complex via an enolate bond in intermediate **45**. The subsequent ring closure occurs in the ground state and is suggested to proceed with high facial diastereoselectivity induced by the chirality of the salen ligand bound to the aluminum center. The dynamics of the process leading from **45** to **43** include an isomerization of the enol double bond and a rotation of the triply substituted radical before or after ISC. The (*S*)-enantiomer is preferred and was found to be the predominant enantiomer in the reaction.

4.2. Sulfoxides

First attempts on the deracemization of chiral sulfoxides were already conducted in the 1970s, albeit with limited success.[49] Recently, a preliminary deracemization procedure for this compound class was disclosed that employed xanthone catalyst *ent*-**40**.[50] A selection of benzothiazinone-1-oxides (*rac*-**46**) was amenable to deracemization under the optimized irradiation conditions (Scheme 27), including different substitutions at the arene core (**46a**–**46c**) as well as at the 3-position (**46d**).

Regarding the mechanism and the nature of a putative achiral intermediate, two potential pathways were considered: the formation of a diradical by C–S bond α-cleavage or a direct inversion of the sulfur stereogenic center. Mechanistic investigations revealed the lability of the C–S bond under sensitization conditions, thus, suggesting α-cleavage being the operative reaction mode. In addition, an energy transfer pathway was energetically feasible based on the triplet energy $E_T = 290\ kJ\,mol^{-1}$ recorded for compound *rac*-**46a** (77 K, MeCN). The relatively low enantioselectivities for sulfoxides **46** were attributed to the marginal difference in steric bulk of the free electron pair and the oxygen atom at the stereogenic center. It was assumed that due to the similarity in size of the substituents, the differentiation between the enantiomers by catalyst *ent*-**40** becomes less pronounced. Both enantiomers were expected to show comparable association behavior and similar triplet energy transfer rates. Nonetheless, the results are valuable because they indicate—together with the cyclopropane studies—that reversible bond cleavage to carbon atoms might be a versatile pathway for deracemization processes.

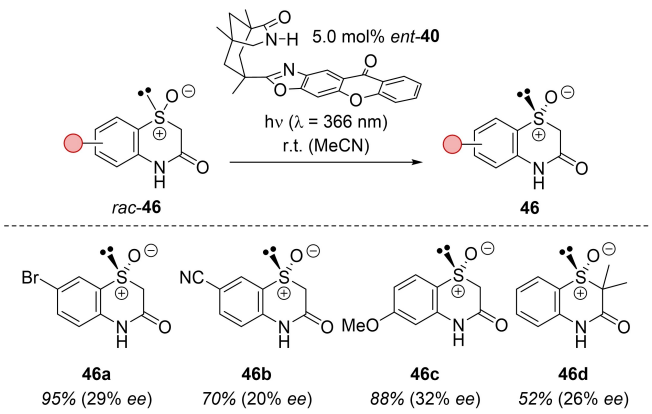

Scheme 27. Catalytic photochemical deracemization of benzothiazin-3(4*H*)-one-1-oxides *rac*-**46** mediated by chiral xanthone ent-**40**: Reaction conditions and a selection of products.

5. Summary and outlook

Photochemical deracemization is a new research topic that holds great potential for the preparation of enantiopure compounds. The reported methods are operationally simple and utilize abundant and benign photons in the wavelength range of λ = 366–500 nm. Despite the impressive progress achieved in the last five years, the substrate scope so far evaluated represents only the tip of the iceberg. In particular, methods which address chiral compounds with a stereogenic carbon atom are expected to be extremely valuable. In this regard, the reversible cleavage of bonds to carbon atoms is of high relevance, irrespective of whether it is induced by energy transfer, electron transfer or hydrogen atom transfer. An understanding of the underlying processes requires synergies between synthesis, computation and spectroscopy, thus providing an excellent platform for interdisciplinary research programs. Our review has provided a glimpse on the current status of photochemical deracemizations that still rely on several preliminary hypotheses, and many open questions remain. Still, we hope it to be useful for those who are fascinated by the tremendous opportunities offered by light-induced reactions.

Acknowledgements

We thank Dr. Liselle Atkin, Dr. Mark Deeprose, and Maximilian Iglhaut (all TU München) for proof-reading the manuscript. TB is indebted to all former and current co-workers involved in photochemical decacemization chemistry (A. Hölzl-Hobmeier, A. Tröster, A. Bauer, A. V. Silva, X. Li, M. Plaza, T. Kratz, A. Seitz, J. Großkopf, S. Breitenlechner, M. Iglhaut, N. Pflaum, B. Boesen, M. Stierle, B. Ghosh, P. Freund, R. Irle) and to our collaboration partners, most notably to Prof. P. Nuernberger (Universität Regensburg), Prof. C. Bannwarth (RWTH Aachen) and Prof. S. M. Huber (Ruhr-Universität Bochum). Our own work in the field was supported by the *Deutsche Forschungsgemeinschaft* (DFG, German Research Foundation) within Collaborative Research Center TRR 325 (project B2), 444632635 and by the Gottfried Wilhelm Leibniz Prize (DFG-1372/23). The *Fonds der Chemischen Industrie* is gratefully acknowledged for a Kekulé fellowship to JG. Open Access funding enabled and organized by Projekt DEAL.

Conflict of Interest

The authors declare no conflict of interest.

Data Availability Statement

Data sharing is not applicable to this article as no new data were created or analyzed in this study.

Keywords: Asymmetric Catalysis · Enantioselectivity · Homogeneous Catalysis · Photocatalysis · Photochemistry

[1] T. Bach, *Angew. Chem. Int. Ed.* **2015**, *54*, 11294–11295.

[2] Reviews: a) P.-Z. Wang, W.-J. Xiao, J.-R. Chen, *Nat. Chem. Rev.* **2023**, *7*, 35–50; b) J. S. DeHovitz, T. K. Hyster, *ACS Catal.* **2022**, *12*, 8911–8924.

[3] Previous reviews on photochemical deracemization: a) J. Wang, X. Lv, Z. Jiang, *Chem. Eur. J.* **2023**, *29*, e202204029; b) Y. Su, Y. Zou, W. Xiao, *Chin. J. Org. Chem.* **2022**, *42*, 3201–3212; c) Q. Shi, J. Ye, *Angew. Chem. Int. Ed.* **2020**, *59*, 4998–5001; d) C. Yang, Y. Inoue, *Nature* **2018**, *564*, 197–199.

[4] W. H. Pirkle, D. S. Reno, *J. Am. Chem. Soc.* **1987**, *109*, 7189–7190.

[5] General reviews on deracemization: a) M. Huang, T. Pan, X. Jiang, S. Luo, *J. Am. Chem. Soc.* **2023**, *145*, 10917–10929; b) H.-J. Gais, *Eur. J. Org. Chem.* **2022**, e202201016; c) C. Aranda, G. Oksdath-Mansilla, F. R. Bisogno, G. de Gonzalo, *Adv. Synth. Catal.* **2020**, *362*, 1233–1257; d) M. Rachwalski, N. Vermue, F. P. J. T. Rutjes, *Chem. Soc. Rev.* **2013**, *42*, 9268–9282; e) N. J. Turner, *Curr. Opin. Chem. Biol.* **2010**, *14*, 115–121; f) S. Servi, D. Tessaro, G. Pedrocchi-Fantoni, *Coord. Chem. Rev.* **2008**, *252*, 715–726; g) C. Gruber, I. Lavandera, K. Faber, W. Kroutil, *Adv. Synth. Catal.* **2006**, *348*, 1789–1805.

[6] Selected examples: a) C. V. Voss, C. C. Gruber, W. Kroutil, *Angew. Chem. Int. Ed.* **2008**, *47*, 741–745; b) A. D. Lackner, A. V. Samant, F. D. Toste, *J. Am. Chem. Soc.* **2013**, *135*, 14090–14093; c) Y. Ji, L. Shi, M.-W. Chen, G.-S. Feng, Y.-G. Zhou, *J. Am. Chem. Soc.* **2015**, *137*, 10496–10499; d) V. Nosek, J. Míšek, *Angew. Chem. Int. Ed.* **2018**, *57*, 9849–9852.

[7] D. G. Blackmond, *Angew. Chem. Int. Ed.* **2009**, *48*, 2648–2654.

[8] For recent work on the photochemical deracemization of a chiral cobalt complex, see: T. A. Schmidt, C. Sparr, *Chem. Commun.* **2022**, *58*, 12172–12175.

[9] Recent examples: a) X. Guo, Y. Okamoto, M. R. Schreier, T. R. Ward, O. S. Wenger, *Chem. Sci.* **2018**, *9*, 5052–5056; b) Z. Zhang, X. Hu, *Angew. Chem. Int. Ed.* **2021**, *60*, 22833–22838; c) J. Wang, Y. Peng, J. Xu, Q. Wu, *Org. Biomol. Chem.* **2022**, *20*, 7765–7769; d) J. D. Williams, P. Pöchlauer, Y. Okumura, Y. Inami, C. O. Kappe, *Chem. Eur. J.* **2022**, *28*, e202200741; e) S. Bierbaumer, L. Schmermund, A. List, C. K. Winkler, S. M. Glueck, W. Kroutil, *Angew. Chem. Int. Ed.* **2022**, *61*, e202117103; f) Q. Chen, Y. Zhu, X. Shi, R. Huang, C. Jiang, K. Zhang, G. Liu, *Chem. Sci.* **2023**, *14*, 1715–1723.

[10] For reviews on deracemization by crystallization, see: a) T. Buhse, J.-M. Cruz, M. E. Noble-Terán, D. Hochberg, J. M. Ribó, J. Crusats, J.-C. Micheau, *Chem. Rev.* **2021**, *121*, 2147–2229; b) A. R. A. Palmans, *Mol. Syst. Des. Eng.* **2017**, *2*, 34–46. For a review on the separation of enantiomers, see: c) H. Lorenz, A. Seidel-Morgenstern, *Angew. Chem. Int. Ed.* **2014**, *53*, 1218–1250.

[11] Recent review: T. Neveselý, M. Wienhold, J. J. Molloy, R. Gilmour, *Chem. Rev.* **2022**, *122*, 2650–2694.

[12] a) O. Rodriguez, H. Morrison, *Chem. Commun.* **1971**, 679; b) C. S. Drucker, V. G. Toscano, R. G. Weiss, *J. Am. Chem. Soc.* **1973**, *95*, 6482–6484.

[13] R. Alonso, T. Bach, *Angew. Chem. Int. Ed.* **2014**, *53*, 4368–4371.

[14] A. Hölzl-Hobmeier, A. Bauer, A. V. Silva, S. M. Huber, C. Bannwarth, T. Bach, *Nature* **2018**, *564*, 240–243.

[15] a) R. Mundt, T. Villnow, C. T. Ziegenbein, P. Gilch, C. Marian, V. Rai-Constapel, *Phys. Chem. Chem. Phys.* **2016**, *18*, 6637–6647; b) N. F. Nikitas, P. L. Gkizis, C. G. Kokotos, *Org. Biomol. Chem.* **2021**, *19*, 5237–5253; c) D. Burget, P. Jacques, *J. Lumin.* **1992**, *54*, 177–181.

[16] H. Gotthardt, G. S. Hammond, *Chem. Ber.* **1975**, *108*, 657–663.

[17] J. Großkopf, T. Kratz, T. Rigotti, T. Bach, *Chem. Rev.* **2022**, *122*, 1626–1653.

[18] a) D. L. Dexter, *J. Chem. Phys.* **1953**, *21*, 836–850; b) N. J. Turro, V. Ramamurthy, J. Scaiano, *Modern Molecular Photochemistry of Organic Molecules*, University Science Books, Sausalito, **2010**, pp. 411–413.

[19] a) G. Bucher, A. A. Mahajan, M. Schmittel, *J. Org. Chem.* **2009**, *74*, 5850–5860; b) M. Plaza, J. Großkopf, S. Breitenlechner, C. Bannwarth, T. Bach, *J. Am. Chem. Soc.* **2021**, *143*, 11209–11217.

[20] M. Plaza, C. Jandl, T. Bach, *Angew. Chem. Int. Ed.* **2020**, *59*, 12785–12788.

[21] a) P. Kapitán, T. Bach, *Synthesis* **2008**, 1559–1564; b) P. Fackler, S. M. Huber, T. Bach, *J. Am. Chem. Soc.* **2012**, *134*, 12869–12878.

[22] Key references: a) Y. Inoue, T. Yokoyama, N. Yamasaki, A. Tai, *Nature* **1989**, *341*, 225–226; b) Y. Inoue, E. Matsushima, T. Wada, *J. Am. Chem. Soc.* **1998**, *120*, 10687–10696; c) Y. Inoue, H. Ikeda, M. Kaneda, T. Sumimura, S. R. L. Everitt, T. Wada, *J. Am. Chem. Soc.* **2000**, *122*, 406–407.

[23] T. Kratz, P. Steinbach, S. Breitenlechner, G. Storch, C. Bannwarth, T. Bach, *J. Am. Chem. Soc.* **2022**, *144*, 10133–10138.

[24] For a review on asymmetric organocatalysis, see: S. Mukherjee, J. W. Yang, S. Hoffmann, B. List, *Chem. Rev.* **2007**, *107*, 5471–5569.

[25] N. Fu, L. Zhang, S. Luo, *Org. Biomol. Chem.* **2018**, *16*, 510–520.

[26] M. Huang, L. Zhang, T. Pan, S. Luo, *Science* **2022**, *375*, 869–874.

[27] J. Saltiel, D. W. L. Chang, E. D. Megarity, A. D. Rousseau, P. T. Shannon, B. Thomas, A. K. Uriarte, *Pure Appl. Chem.* **1975**, *41*, 559–579.

[28] T. Hofbeck, H. Yersin, *Inorg. Chem.* **2010**, *49*, 9290–9299.

[29] F. Lovering, J. Bikker, C. Humblet, *J. Med. Chem.* **2009**, *52*, 6752–6756.

[30] *Visible Light Photocatalysis in Organic Chemistry* (Eds.: T. P. Yoon, C. R. Stephenson, D. W. C. MacMillan), Wiley-VCH, Weinheim, **2018**.

[31] N. Y. Shin, J. M. Ryss, X. Zhang, S. J. Miller, R. R. Knowles, *Science* **2019**, *366*, 364–369.

[32] Reviews: a) R. Cano, A. Zakarian, G. P. McGlacken, *Angew. Chem. Int. Ed.* **2017**, *56*, 9278–9290; b) D.-Q. Dong, S.-H. Hao, Z.-L. Wang, C. Chen, *Org. Biomol. Chem.* **2014**, *12*, 4278–4289; c) F. Bellina, R. Rossi, *Chem. Rev.* **2010**, *110*, 1082–1146.

[33] Reviews: a) J. Cao, S.-F. Zhu, *Bull. Chem. Soc. Jpn.* **2021**, *94*, 767–789; b) L. Duhamel, P. Duhamel, J. C. Plaquevent, *Tetrahedron: Asymmetry* **2004**, *15*, 3653–3691; c) C. Fehr, *Angew. Chem. Int. Ed.* **1996**, *35*, 2566–2587.

[34] C. Zhang, A. Z. Gao, X. Nie, C.-X. Ye, S. I. Ivlev, S. Chen, E. Meggers, *J. Am. Chem. Soc.* **2021**, *143*, 13393–13400.

[35] P. S. Steinlandt, W. Zuo, K. Harms, E. Meggers, *Chem. Eur. J.* **2019**, *25*, 15333–15340.

[36] L. Konnert, F. Lamaty, J. Martinez, E. Colacino, *Chem. Rev.* **2017**, *117*, 13757–13809.

[37] A. Bauer, F. Westkämper, S. Grimme, T. Bach, *Nature* **2005**, *436*, 1139–1140.

[38] a) J. Großkopf, M. Plaza, A. Seitz, S. Breitenlechner, G. Storch, T. Bach, *J. Am. Chem. Soc.* **2021**, *143*, 21241–21245; b) R. J. Kutta, J. Großkopf, N. van Staalduinen, A. Seitz, P.

Pracht, S. Breitenlechner, C. Bannwarth, P. Nuernberger, T. Bach, *J. Am. Chem. Soc.* **2023**, *145*, 2354–2363.
[39] Z. Gu, L. Zhang, H. Li, S. Cao, Y. Yin, X. Zhao, X. Ban, Z. Jiang, *Angew. Chem. Int. Ed.* **2022**, *61*, e202211241.
[40] Reviews: a) J. Bergman, *Adv. Heterocycl. Chem.* **2015**, *117*, 1–81; b) G. M. Ziarani, P. Gholamzadeh, N. Lashgari, P. Hajiabbasi, *Arkivoc* **2013**, 470–535; c) G. M. Karp, *Org. Prep. Proced. Int.* **1993**, *25*, 481–513; d) W. C. Sumpter, *Chem. Rev.* **1945**, *37*, 443–479.
[41] J. Großkopf, A. A. Heidecker, T. Bach, *Angew. Chem. Int. Ed.* **2023**, *62*, e202305274.
[42] a) G. S. Hammond, R. S. Cole, *J. Am. Chem. Soc.* **1965**, *87*, 3256–3257; b) S. L. Murov, R. S. Cole, G. S. Hammond, *J. Am. Chem. Soc.* **1968**, *90*, 2957–2958.
[43] C. Ouannès, R. Beugelmans, G. Roussi, *J. Am. Chem. Soc.* **1973**, *95*, 8472–8474.
[44] A. Tröster, A. Bauer, C. Jandl, T. Bach, *Angew. Chem. Int. Ed.* **2019**, *58*, 3538–3541.
[45] X. Li, R. J. Kutta, C. Jandl, A. Bauer, P. Nuernberger, T. Bach, *Angew. Chem. Int. Ed.* **2020**, *59*, 21640–21647.
[46] A. Brown, F. Wilkinson, *J. Chem. Soc. Faraday Trans. 2* **1979**, *75*, 880–895.
[47] F. Burg, T. Bach, *J. Org. Chem.* **2019**, *84*, 8815–8836.
[48] C. Onneken, T. Morack, O. Sokolova, N. Niemeyer, C. Mück-Lichtenfeld, C. G. Daniliuc, J. Neugebauer, R. Gilmour, *Nature* **2023**, https://doi.org/10.1038/s41586-023-06407-8.
[49] G. Balavoine, S. Jugé, H. B. Kagan, *Tetrahedron Lett.* **1973**, *14*, 4159–4162.
[50] L. Wimberger, T. Kratz, T. Bach, *Synthesis* **2019**, *51*, 4417–4424.

Manuscript received: June 12, 2023
Accepted manuscript online: July 10, 2023
Version of record online: September 19, 2023